National Transportation Safety Board
Office of Research and Engineering
Washington, DC 20594

ERA23FA174

MATERIALS LABORATORY

Factual Report 23-051

May 16, 2024

(This page intentionally left blank)

A. ACCIDENT INFORMATION

Location: Gulf of Mexico, GM
Date: March 30, 2023
Vehicle: Cessna 525B, N869AC
Investigator: Clinton R. Crookshanks, AS-40

B. COMPONENTS EXAMINED

Winglet and portion of wing extension designed by Tamarack Aerospace Group, Inc.

C. EXAMINATION PARTICIPANTS

Specialist	Michael Meadows National Transportation Safety Board Washington, District of Columbia
Group Chair / IIC	Heidi Kemner National Transportation Safety Board Washington, District of Columbia
Group Chair	Clinton R. Crookshanks National Transportation Safety Board Aurora, Colorado
Specialist	Adam Huray National Transportation Safety Board Washington, District of Columbia
Party Coordinator	Hal Gates Tamarack Aerospace Group Sandpoint, Idaho
Group Member	Danny Pfeifer Tamarack Aerospace Group Sandpoint, Idaho
Party Coordinator	Kurt Gibson Textron Aviation Wichita, Kansas
Group Member	Joseph Hodgin Federal Aviation Administration Seattle, Washington

D. DETAILS OF THE EXAMINATION

On March 30, 2023, a Cessna 525B, N869AC, was substantially damaged when it was involved in an accident over the Gulf of Mexico. The pilot reported that he noticed the left winglet had separated from the wing after feeling two "big jolts" and a yaw while in a cruise descent at an altitude of approximately 30,000 feet. The pilot subsequently performed an emergency landing at Tampa International Airport (TPA), Tampa, Florida, without issue. No injuries were reported, but the left winglet had departed the aircraft, and the left wing-extension component was substantially damaged. The airplane was operated as a Title 14 Code of Federal Regulations Part 91 corporate flight.

A portion of the left wing-extension assembly which remained attached to the accident airplane along with a portion of the left winglet assembly recovered from the Gulf of Mexico 11 days after the event, were submitted to the NTSB Materials Laboratory (Washington, D.C.) for examination. The Tamarack Active Control Surface (TACS) portion of the wing extension assembly was not recovered. A group examination of the submitted evidence was conducted at the NTSB Materials Laboratory from 13 – 15 June 2023 with the participants listed in the above section.

Figure 1 shows photographs of the right winglet, wing extension assembly, and TACS assembly which remained attached to the accident airplane. The damaged left-hand components were mirrored designs and are the focus of this report. The wing extension, TACS, and composite winglet assemblies are designed to be installed on the outboard end of the original equipment manufacturer (OEM) wing.

An ultraviolet (UV) light inspection was performed on the submitted components to identify presence of any organic contaminants and no relevant indications were observed.

Figure 2 shows inboard and outboard views of the winglet, an assembled fiber reinforced polymer matrix composite structure, which was still attached to the winglet attachment rib component of the wing extension assembly. The wingtip light assembly and glare shield components were still attached, and the static wicks and their associated bases had separated from the inboard skin surface. The outboard TACS hinge support brackets and portions of the outboard TACS hinge brackets (fractured), upper and lower main spar caps (fractured), main spar web (fractured), forward spar web (fractured), and lower skin (fractured) were still attached to the winglet attachment rib. The winglet assembly ID placard contained the following part identification information:

Tamarack Aerospace Group
Part Number: 103-57-1700-01
Revision: K

Serial Number: 01003
Supplier Ident: 5VTA5[1]

Figure 3 shows a view of the lower surface of the winglet. Several white scratches were observed on the blue painted area of the lower surface. White powdery deposits were observed around some of the fasteners and metallic surfaces, consistent with corrosion and deposits from exposure to a marine environment. A portion of the lower skin from the wing extension assembly remained attached to the winglet attachment rib.

Figure 4 shows an area of localized damage to the upper inboard corner of the winglet, located just aft of the winglet attachment rib and just outboard of the outboard TACS hinge brackets. Damage signatures consisted of chipped paint, crushed carbon fibers, and interlaminar separation. A crack, approximately 3.7 inches long, was observed extending between the forward end of the winglet closeout and upper skin. Similar cracks were observed in the paint layer extending approximately 4.7 inches from the forward end of the winglet closeout at the lower skin joint. A Z-shaped shear clip which connected to the inner surface of the winglet closeout and the winglet attachment rib was partially separated from the closeout, as indicated in figure 4. A mirror was used to visually examine the forward face of the shear clip leg which spanned between the attachment flanges as shown in figure 5. This leg exhibited outboard deformation and buckling. The damage to the winglet closeout, upper skin, and shear clip was consistent with localized impact or mechanical contact damage to the closeout near the upper skin edge.

Figure 6 shows a photo of the outboard side of the winglet tip where an area of red material transfer, inconsistent with the aircraft exterior livery, was observed. The transfer mark was approximately 3 inches in length and was located along the outboard tangent of the rounded winglet tip as indicated by the red bracket and shown more closely in the right image. The overall appearance was a series of colinear streaks with smaller smeared streaks emanating downward and slightly aft. A specimen of the red material was extracted for chemical analysis using Fourier transform infrared (FTIR) spectroscopy and the spectrum was consistent with a polyurethane chemistry typically found in aircraft topcoats and industrial paints and was indistinguishable from the white topcoat material.

The glare shield, a fiber reinforced polymer composite component, remained attached to the winglet and exhibited localized damage signatures as shown in the left image of figure 7. Two areas of crushed fibers were observed on the inboard edge of the glare shield as indicated by yellow arrows, with the area on the upper surface located approximately 5.5 inches aft of the apex of the leading edge, and the

[1] The Commercial and Government Entity (CAGE) code corresponded to Blackhawk Composites, Inc., Morgantown, KY (Source: https://cage.dla.mil)

area on the lower surface located approximately 0.9 inch aft of the apex of the leading edge, near the lower tip of the winglet rib fitting. A witness mark, indicated by a red arrow, was observed on the inboard vertical surface of the glare shield which emanated towards an area of chipped paint on the upper edge. The upper right image of figure 7 shows the inboard side of the glare shield after disassembly and yellow brackets indicate areas of chipped paint near the crushed fibers along the inboard edge and areas of chipped paint on the upper edge. The lower right image of figure 7 shows a closer view of the boxed area along the upper inboard edge and adjacent faying surface where crushed fibers were observed. Interlaminar cracks emanated from the crushed fibers and residual fractured sealant was observed on the adjacent surface, as indicated by white arrows.

Figure 8 shows a view of the portion of the wing extension assembly that was received. The leading edge had been disassembled from the forward spar and splice joints. The upper skin and a majority of the lower skin were not received. The fractured TACS tube (long pushrod) was reportedly disassembled from the bellcrank to facilitate removal from the OEM wing and was received installed forward of the main spar, as pictured, rather than through the main spar as specified in installation drawings. On scene photos, prior to removal from the accident airplane, showed the tube oriented aft through the main spar pass-through as intended by design and as shown in the following figure.

E. MAIN SPAR FRACTURE, INBOARD LOCATION

Figure 9 shows views looking inboard along the fractured main spar of the wing extension assembly, just outboard of the bellcrank mechanism. The main spar, which consisted of upper and lower T-shaped caps fastened to a vertical web, was fractured transversely just outboard of the attached bellcrank fitting. The upper and lower main spar caps were fractured through the stem at the outboard fasteners where the bellcrank bracket attached. Closer views of these areas within the yellow boxes are shown in figure 10. The lower spar cap flange was fractured slightly outboard from the stem through a fastener hole where the lower skin attached, approximately 7 inches from the inboard end of the wing extension assembly. The top flange of the upper main spar cap was fractured approximately 7.1 inches from the inboard end of the wing extension assembly, between upper skin fastener locations, and exhibited deformation and shear lip features consistent with overstress separation. The top flange of the upper main spar cap was partially separated and deformed upward away from the stem with shear lip features across the fracture surface, consistent with overstress separation under peel loading. The main spar web extended approximately 1 inch outboard from the spar cap stem fractures where it was fractured through the next set of fastener holes and bent aft. The fracture surface of the main spar web exhibited shear lip features, consistent with tensile overstress separation. Witness marks in the form of scraped primer and parallel scratches/gouges, consistent with mechanical contact damage, were observed on the

forward side of the main spar web extending from the cap stem fractures to the web fracture. The witness marks were contained within regions approximately 0.75 inch from the upper and lower edges of the web as indicated by red brackets, consistent with contact with the upper and lower spar cap stems. The inboard main spar cap fracture surfaces were sectioned from the assembly to facilitate closer examination, and observations are detailed later in this report.

F. MAIN SPAR FRACTURE, OUTBOARD LOCATION

The main spar caps (upper and lower) were fractured transversely through the T-shaped cross section through the fastener holes approximately 1 inch inboard of the edge of the winglet attachment rib as shown in figure 11. The transverse fractures turned outboard along the forward side of both flanges and continued to the outboard edges of the caps. The main spar web was fractured along the same plane through the same fastener holes and exhibited shear lip features, consistent with tensile overstress separation. Contact marks, indicated by red arrows, were observed on the upper and lower inboard edges of the winglet attachment rib approximately 1.4 inches forward of the main spar. The outboard main spar cap fracture surfaces were sectioned from the assembly to facilitate closer examination, and observations are detailed later in this report.

The portions of the upper and lower main spar caps and web between the inboard and outboard fracture locations were not recovered and therefore not examined.

G. TACS ASSEMBLY & ATTACHMENT

The TACS assembly was not recovered, and therefore not examined. The TACS assembly attached to the aft side of the main spar at two locations via two lapped hinge brackets, each sandwiched between inboard and outboard bent sheet metal support brackets. The inboard TACS hinge brackets attached at the outboard end of the bellcrank bracket. Remnants of the fractured support brackets were retained at the fastener locations and were deformed aft away from the main spar web as indicated in the right image of figure 9. The fracture surfaces exhibited shear lip features consistent with overstress separation. The TACS Tube Assembly was fractured near the aft end in the threaded portion and the fracture surface exhibited shear lip features and necking deformation consistent with tensile overstress separation. The TACS tube was disassembled from the bellcrank for closer examination. Figure 12 shows photographs of the outboard and inboard sides of the TACS tube relative to a straight edge. Small gaps were observed near the center of the outboard side and at each end of the inboard side, consistent with a slight inboard bow. No appreciable gaps were observed along the upper and lower sides of the tube. The tube was 3D scanned using a Keyence VL-500 series optical scanner and contour maps were generated along the constant diameter portion of the tube to

measure the outer surface radius relative to a best fit cylinder axis.[2] The deflections observed agreed with the straight edge comparison. From the 3D scan data, straightness of the constant diameter section of the tube was estimated to be within 0.007 inch, which was within specified engineering tolerances. The outboard TACS hinge and support brackets were still attached to the winglet attachment rib and lower skin remnant, and partially attached to the aft side of the main spar. The outboard TACS hinge brackets were bent inboard and fractured through the lower-aft quadrant of the lug, with the upper ligaments deformed aft as shown in figures 13 and 14, highlighted by yellow arrows. The web of the outboard hinge support bracket (outboard TACS hinge location) was deformed inboard and partially torn at the upper-aft fastener location and bend radius at the aft edge of the upper flange as shown in the right image of figure 13. The upper flange of the inboard hinge bracket (outboard TACS hinge location), which attached to the upper skin, was deformed upwards and the forward flange was deformed aft, separated from the aft side of the main spar, with a portion of a fractured rivet retained in the upper attachment hole.

H. FORWARD SPAR FRACTURE

The forward spar web was fractured through the forward set of fastener holes which attached to the winglet attachment rib as indicated in figure 14. The portion of the forward spar web still attached to the accident airplane was plastically deformed and bent aft and downward with the 20 outboard-most fasteners separated from the lower forward spar cap as shown in figure 15, indicated by a yellow bracket. The four circled holes at the inboard spar cap-to-web joints contained fasteners that were removed to aid with disassembly from the accident airplane and no appreciable separation of the web-to-spar cap faying surfaces was observed. The 2 outboard most fasteners and the 2 fasteners just outboard of the weight reduction holes where the forward spar web attached to the upper forward spar cap were separated. The web was partially fractured from the lower surface to the bottom of the outboard weight reduction hole and deformed aft above the outboard weight reduction hole at the location indicated by the red arrow in figure 15, consistent with compressive buckling or torsion loading. The upper and lower forward spar caps were splayed open and partially separated from the leading edge splice joints at the outboard end, consistent with aft bending and/or outward loading on the upper and lower surfaces.

I. LEADING EDGE DAMAGE AND FRACTURE

The C-shaped leading edge component was received disassembled from the wing extension assembly as shown in the upper image of figure 16. The chemical composition of the leading edge component was consistent with a 6XXX series aluminum alloy as identified using x-ray fluorescence (XRF) spectroscopy. The leading edge was partially fractured chordwise along the upper surface through the second

[2] The contour map scale was based on a nominal diameter of 0.506 inch measured using calipers. This measurement included primer and paint layers.

fastener hole, approximately 3 inches from the outboard edge. The fracture terminated at the lower surface near the apex of the leading edge as indicated by a red arrow, and the outboard section was bent downward and plastically deformed. The deformed shape of the outboard end of the leading edge matched the profile of the forward end of the winglet attachment rib and witness marks on the inner surface of the leading edge were consistent with contact with the forward end of the winglet attachment rib. A linear streak was observed at the outboard end of the leading edge upper surface which spanned between the white arrows in the lower image of figure 16. The streak consisted of parallel scratches oriented slightly off axis from the chordwise direction as shown in the inset image in figure 16. Two areas of yellow material transfer were observed within the parallel scratches as indicated by yellow arrows. Elevated levels of strontium were detected at these regions using XRF spectroscopy, consistent with a common constituent of chromated primer coatings. Abrasions and scratches were also observed on the upper surface of the leading edge in the area indicated by a green bracket. The outboard fastener holes on the leading edge were enlarged as shown in figure 17, and the lower hole was torn inward consistent with the countersink fastener head pulling through during separation from the winglet attachment rib. The upper fastener hole was elongated between approximately 0.20 – 0.65 inch from the aft edge and deformed forward and slightly outboard relative to the original fastener hole. The lower fastener hole was elongated to approximately 0.60 inch from the aft edge. All other intact leading edge fastener hole locations measured approximately 0.26 and 0.55 inch from the aft edge of the leading edge to the aft and forward edges of the countersunk fastener heads, respectively. The lower outboard leading edge fastener remained secured by the respective nutplate on the winglet attachment rib. The upper outboard leading edge fastener head was fractured and not recovered.

Witness marks, consistent with mechanical contact damage, were observed at the outboard end of the leading edge (inner surface), forward spar, and winglet attachment rib as detailed in figures 17 – 24. The inner surface of the leading edge exhibited white, yellow, and dark gray material transfer marks, consistent with contact with the forward end of the winglet attachment rib, shown in figure 19. Corresponding areas of disturbed and chipped primer were observed on the forward end of the winglet attachment rib. Contact marks were observed on the inboard edge of the winglet attachment rib, indicated by red arrows in figure 20, which shows the upper forward edge of the attachment rib aligned with the inboard contact mark observed on the inner surface of the leading edge. The lower inboard edge of the rib exhibited upward deformation near the contact marks. The mark observed at the upper inboard edge of the rib was consistent with contact with the outboard end of the upper leading edge splice joint. When these features were aligned, as shown from below and above in figures 21 and 22, respectively, the fractured lower forward spar cap interfered with the lower surface of the winglet attachment rib. When the upper forward edge of the attachment rib was aligned with the outboard contact mark observed on the inner surface of the leading edge, as shown in figure 23 (the

outboard portion of the deformed forward spar was removed for clarity), locations of contact marks and deformation observed on the lower inboard edge of the attachment rib corresponded with contact marks observed on the outboard end of the lower forward spar cap as indicated by red arrows. Additional contact marks were observed on the lower side of the upper leading edge splice and the forward side of the upper forward spar cap, which was bent back and downward as shown in figures 21 and 24 (red arrows). A gouge was observed on the forward side of the forward spar web, as indicated by a red arrow, which corresponded to dragging contact with the outboard end of the upper forward spar cap, which was bent aft and upward.

J. WING EXTENSION SKIN RIVET FRACTURES

The upper skin and a majority of the lower skin from the wing extension assembly were not recovered. Fractured rivets were observed at the joints where the skins attached to the leading edge splice joints, main spar caps, winglet attachment rib, and OEM wing closeout. The schematics shown in figures 25 – 28 detail locations where fasteners were observed intact (filled circle), fractured (open circle), and missing (circle with inscribed "X"). The letters below fractured fasteners correspond to shear fracture mode (S), tensile fracture mode (T), or mixed mode bending fracture (T/B, S/B).

Along the leading edge splice joint, all fasteners were present and intact with the exception of the three outboard most fasteners on the upper surface and the second outboard most fastener on the lower surface (dashed circle in figure 26), which had been drilled out for disassembly prior to receipt by NTSB. The outboard lower leading edge fastener was still retained in the nutplate on the winglet attachment fitting. The upper and lower inboard most fasteners were also not present but the countersunk holes in the leading edge component did not appear damaged or deformed. A total of 23 fastener locations were observed where the upper skin attached to the upper leading edge splice and forward spar cap. Of these locations, 16 fasteners exhibited tensile overstress fracture features, 3 fasteners exhibited shear overstress fracture features, 3 exhibited mixed tensile/shear and bending fractures, and 1 fastener was missing. A total of 23 fastener locations were observed where the lower skin attached to the lower leading edge splice and forward spar cap. All of these fasteners exhibited tensile overstress fractures except the outboard most fastener, which was missing.

There were 10 fastener locations along the upper surface of the winglet attachment rib where the upper skin and leading edge attached. Of these locations, 3 fasteners exhibited tensile fractures, 2 exhibited shear fractures, 3 exhibited bending or mixed bending shear/tensile fractures, and 2 were missing as indicated in figure 27. The fasteners along the lower surface of the winglet attachment rib, where the lower skin attached, were still intact with a portion of the lower skin retained. The forward fastener where the leading edge attached was bent but still intact and

retained in the winglet attachment rib. The portion of retained lower skin was fractured forward of the main spar location, deformed downward away from the winglet attachment rib, and exhibited shear lip fracture features along the inboard edge, consistent with overstress separation. The portion of retained lower skin exhibited upward bending deformation just aft of the main spar where connected to the outboard TACS hinge bracket.

The inboard portion of the wing extension assembly contained 18 fastener locations on the upper and lower sides where the upper and lower skins were attached as shown in figure 28. All of these fasteners exhibited tensile overstress fractures except the outboard most fastener on the lower surface which was missing, and also coincided with the inboard lower main spar cap fracture as shown in the right image of figure 28. The fastener locations bounded by red boxes were drilled out prior to the NTSB Materials Laboratory examination to aid with disassembly from the accident airplane.

Examples of typical rivet fractures are shown in figure 29 with solid rivet tensile/bending fractures shown on the left, a blind rivet tensile fracture shown in the upper right, and a solid rivet shear fracture shown in the lower right.

K. BELLCRANK MECHANISM CONNECTIONS

The bellcrank mechanism and connections were visually examined from the walking beam component to the fractured TACS tube component as identified in figure 8. Flanged bushings were observed installed in all walking beam holes. The walking tube (short pushrod) assembly was installed to the walking beam fitting at the pivot point and the installed cotter pin was intact. The lock wires at the inboard and outboard jam nuts on the short pushrod assembly were intact. The short pushrod assembly was connected to the bellcrank. The bellcrank and spring assembly was attached to the bellcrank bracket about the pivot point and via the TACS return bracket with lockwire about the jam nut and TACS return bracket still intact. As received, the bellcrank had approximately 0.23 inch range of motion between aft contact with the bushing installed through the bellcrank bracket and forward movement restricted by the spring when engaged with the screw and spherical washers attached to the TACS return bracket. Range of motion was measured along the TACS return bracket fail stop edge, indicated by two horizontal black lines in the right image of figure 31. Light vertical contact marks were observed on the bellcrank which closely matched the position of the forward side of the bushing and the aft side of the TACS return bracket as indicated by a red arrow in figures 30 and 31.

L. SPAR CAP FRACTOGRAPHY

The fractured main spar caps at the outboard end of the bellcrank bracket (inboard main spar fracture location) were sectioned from the wing extension

assembly and disassembled from the bellcrank bracket and main spar web for closer examination of the fracture surfaces as shown in figure 32. The upper main spar cap fracture surface was smeared, with a greater degree of smearing on the upper side of the fastener hole.

A scanning electron microscope (SEM) was used to examine fracture features on the spar caps more closely. The lower main spar cap exhibited fracture initiation sites at the lower surface, opposite of the stem-to-flange junction as indicated by yellow arrows in figure 33. These radial marks emanated from an area of parallel streaks on the adjacent lower surface over a region which extended upward into the part approximately 0.01 inch as indicated by black dashed arrows, over a relatively flat plane before transitioning to rougher fracture features and smearing damage. The streaks observed on the adjacent lower surface were consistent with machining marks or surface patterns generated during an extrusion process. Figure 34 shows a typical example of the fracture initiation area at higher magnification using a secondary electron detector. Dimpled features were observed interspersed with islands of linear striated features, oriented horizontally in these images, and the fracture mode was consistent with overstress dominated tensile or upward bending fracture.

A secondary crack was observed along the forward flange of the lower main spar cap at the inboard fracture location through the next outboard lower skin fastener location as indicated by a red bracket in figure 32. The flange was deformed downward, and the fracture surface exhibited shear lip features consistent with overstress separation. The aft flange of the lower main spar cap exhibited smearing damage and shear lip features on the fracture surface and was buckled, consistent with compressive loading and overstress separation. The upper part of the lower main spar cap stem fracture surface above the fastener hole exhibited a smeared and battered appearance consistent with post separation contact damage as shown more closely in figure 35.

The appearance of the lower main spar fracture surface at the inboard location around the main spar web/bellcrank fitting fastener hole location were examined more closely as shown in figures 36 – 40. These areas were smeared and exhibited mechanical contact damage. Just below the fastener hole (figures 36 and 37), dimpled fracture features were observed at higher magnification where smearing was less prevalent, as shown in the scanning electron microscope image in figure 37, consistent with overstress fracture. Just above the fastener hole, as shown in figure 38, smearing and contact damage was observed adjacent to the hole. The central fractured region as shown in the SEM image exhibited a rough dimpled appearance with shear lip features and necking deformation observed on the right and left side of the spar cap stem, consistent with overstress separation. Closer views of the boxed area in the SEM image are shown in figures 39 and 40, which was above an area where mechanical contact/smearing damage was observed. This area exhibited

striated features (oriented horizontally in the images) interspersed with dimpled features.

The fractured main spar caps at the inboard end of the winglet attachment rib (outboard main spar fracture location) were disassembled from the attachment rib, main spar web, and outboard TACS hinge bracket supports for closer examination. Views of the spar caps as disassembled are shown in figure 41. Figure 42 shows a view of the fracture surfaces tilted slightly aft. The fracture path along the spar cap stems was oriented along a chordwise plane transverse to the wing axis. The fracture surface in the vicinity of the fastener holes was smeared, consistent with mechanical contact damage. The aft flanges exhibited smeared shear lip features, consistent with overstress separation. The forward flanges of both main spar caps were fractured from the stem fracture surface to the outboard end of the part. The lower spar cap forward flange fracture surface extended along a forward angled path and exhibited a shear lip, consistent with overstress separation. The upper spar cap forward flange fracture surface extended along the wing axis and was relatively rough in appearance.

Figure 43 shows scanning electron microscope images (right) of a region of flat fracture on the lower main spar cap stem in the area highlighted by the yellow box in the left image. The upper right image was taken after ultrasonic cleaning the fracture surface using a mild detergent followed by acetone. The surface exhibited a mudcracked appearance consistent with oxide layer buildup from extended exposure to a marine environment which obscured any visible fracture features. Progressive cleaning techniques including acetate tape replicas and additional ultrasonic solvent cleanings did not sufficiently remove the oxide layer, so a heated chromic-phosphoric acid cleaning procedure was then used to remove the oxide layer. The lower right image shows the same area following the heated acid cleaning procedure. After acid cleaning, the surface was relatively smooth and featureless and fracture features were not observable, consistent with smearing from mechanical contact damage or fracture features being consumed by the built up oxide layer.

Figure 44 shows a secondary electron image (right), following the heated acid cleaning procedure, of a region of flat fracture on the upper main spar cap in the area highlighted by the yellow box in the left image. Remnants of the oxide layer were observed over a dimpled subsurface, consistent with microvoid coalescence and overstress separation.

Figure 45 shows a secondary electron image of the fracture surface of the forward flange of the upper main spar cap after ultrasonic cleaning using a mild detergent followed by acetone (prior to the heated acid etch). A similar mudcracked oxide layer appearance was observed, however a dimpled appearance was observed beneath the oxide layer, consistent with overstress separation.

M. CHEMICAL AND PHYSICAL PROPERTY EVALUATION

The components listed in Table I were pieces of the primary structure which were observed to be fractured. Component thicknesses were measured using digital calipers and micrometers. Chemical analysis was performed using x-ray fluorescence spectroscopy (XRF) and all components were consistent with 2XXX series aluminum alloys. Electrical conductivity and hardness measurements were performed on each component in accordance with Aerospace Material Specification 2658 and measured values are tabulated in Table I. All components were within expected ranges for the material form and temper condition specified.

A stringlike substance was observed on the accident vehicle airplane on the outboard static wick base on the underside of the left-wing aileron adjacent to a region of residue. This material was analyzed using energy dispersive x-ray spectroscopy (EDS) and FTIR spectroscopy and the spectra for the stringlike substance were consistent with a polysulfide chemistry typically found in aircraft sealants. The spectra from a swabbed sample of the residue were inconclusive and only positively identified cellulose from the swab material.

An orange grease like substance was observed on the outboard side of the outboard TACS hinge and support brackets and winglet closeout where local impact damage on the winglet was observed (see figures 4 and 13). This material was analyzed using FTIR spectroscopy and the chemistry was consistent with typical lubricants used in bearing applications such as MIL-G-81322.

Submitted by:

Michael Meadows
Materials Engineer

Table I: Chemical and Physical Properties of Fractured Components

Part Identification	Electrical Conductivity (% IACS)	Hardness (HRB)	Thickness (in)	Chemistry (XRF)
CAP, MAIN SPAR, UPPER	29.7	76.6	0.080	Consistent with 2XXX series aluminum alloys
CAP, MAIN SPAR, LOWER	29.5	78.8	0.079	
WEB, MAIN SPAR	32.4	69.0	0.052 [1]	
WEB, FWD SPAR	32.1	62.8	0.054	
BRACKET, TACS HINGE, OUTBD (OUTBOARD)	30.1	78.2	0.215	
BRACKET, TACS HINGE, OUTBD (INBOARD)	29.9	76.3	0.214	
SKIN, LOWER	31.3	73.7	0.083 [1]	
ASSY, TUBE, TACS FREEMAN	23.9	76.3 [2]	0.065 [3]	

Notes:
[1] Thickness measurement includes paint/primer layer.
[2] Hardness value was corrected for a cylindrical specimen with an outside diameter of 0.4975 inch.
[3] Thickness measurement of nominal tube thickness. Fracture occurred in threaded area with necking deformation.

Figure 1. Photographs of the right winglet and wing extension which remained attached to the accident airplane.

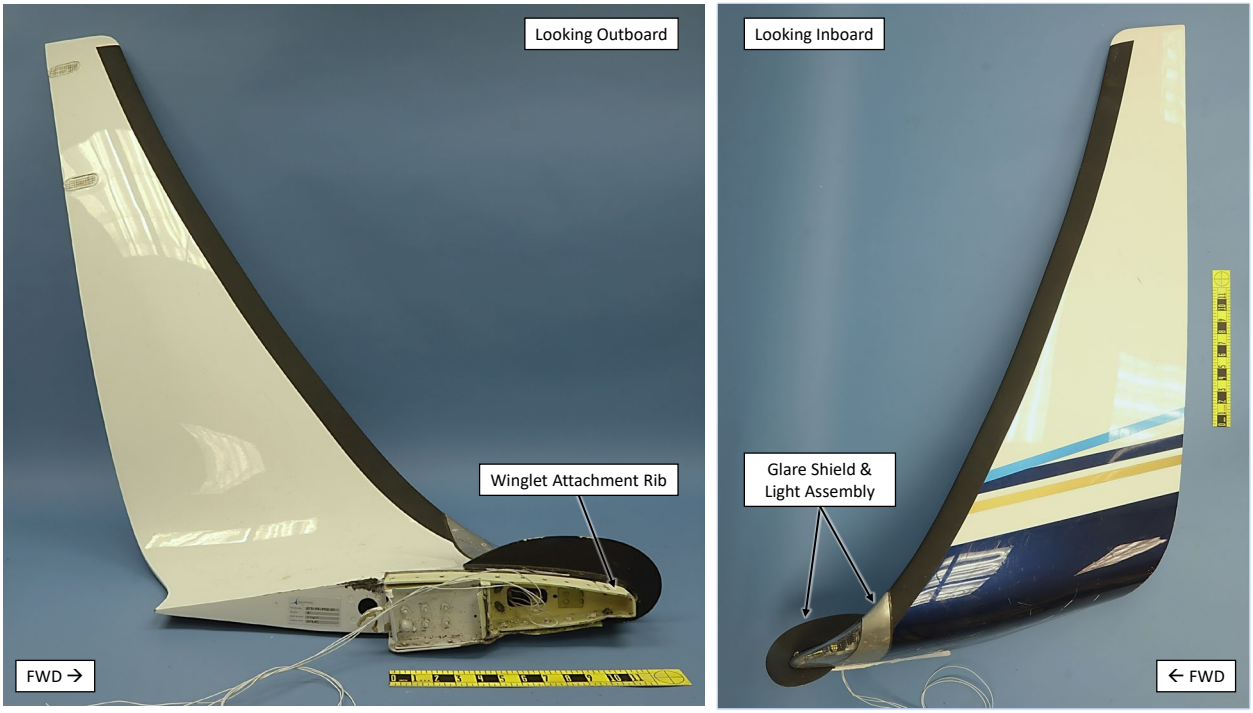

Figure 2. Photographs of the left winglet as received.

Figure 3. Photograph of the left winglet lower surface as received.

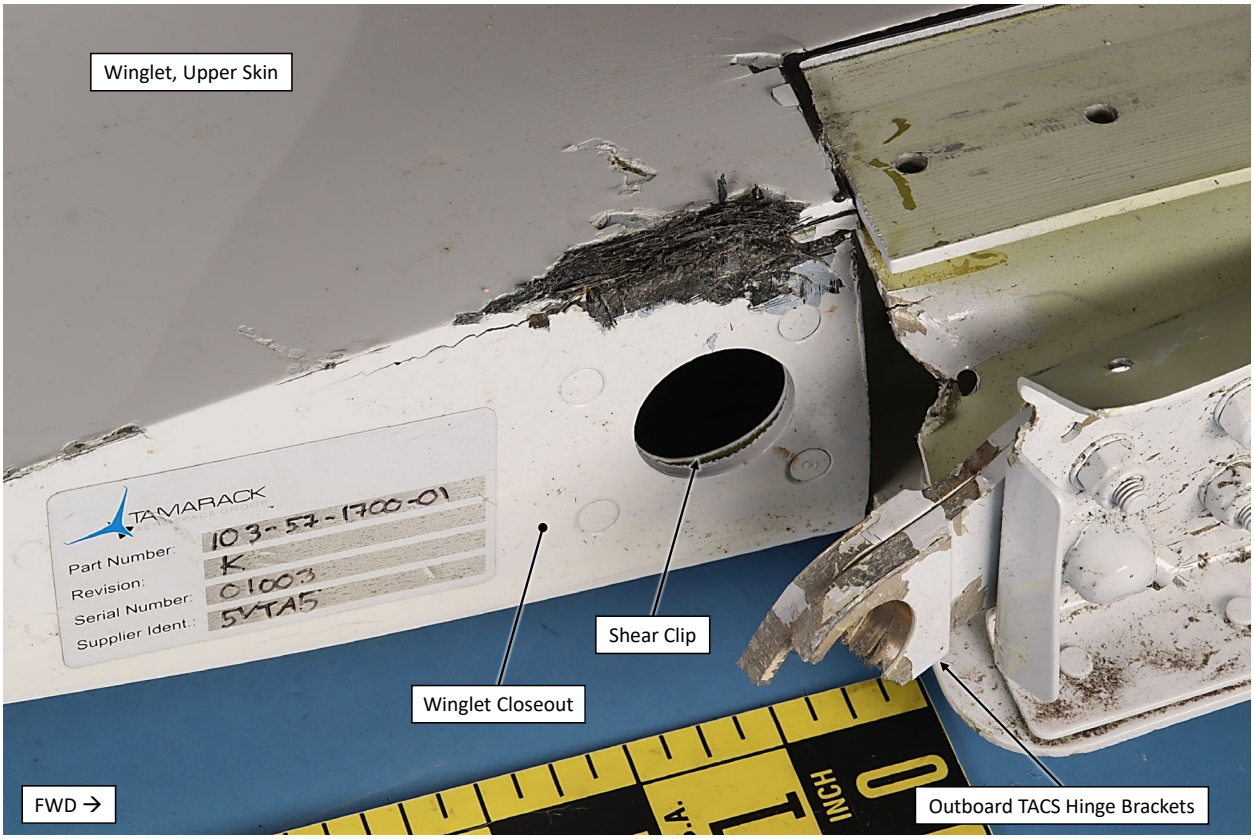

Figure 4. Photograph showing localized damage to the composite construction of the left winglet, aft of the winglet attachment rib and outboard of the TACS hinge brackets.

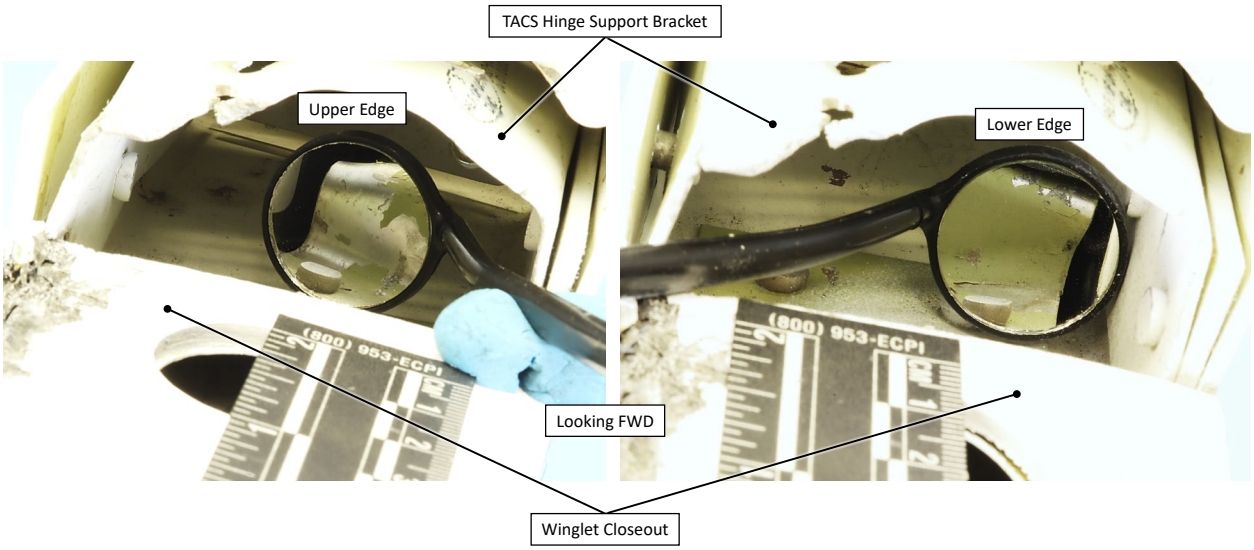

Figure 5. Photographs showing deformation to the forward-facing surface of the shear clip component as viewed in an inspection mirror.

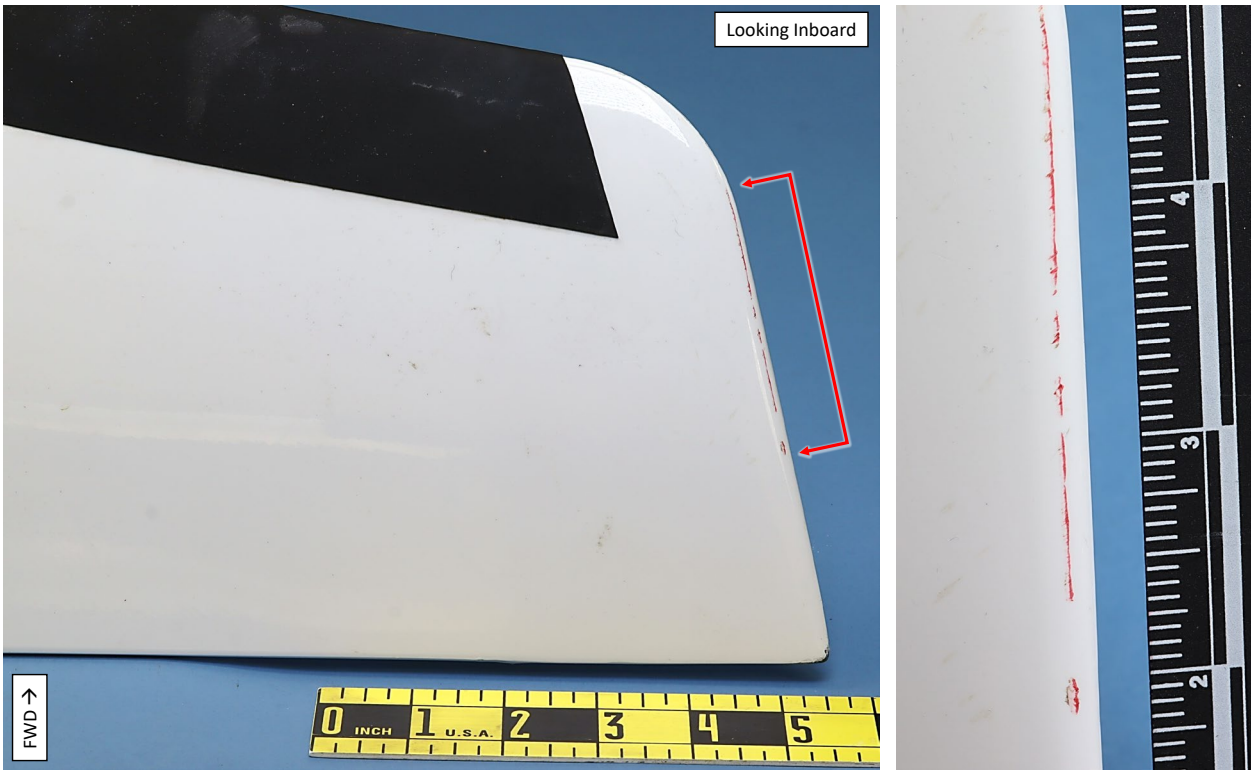

Figure 6. Photograph of an area of red material transfer observed on the outboard side of the winglet tip indicated by the red bracket. A closer view of this area is shown on the right.

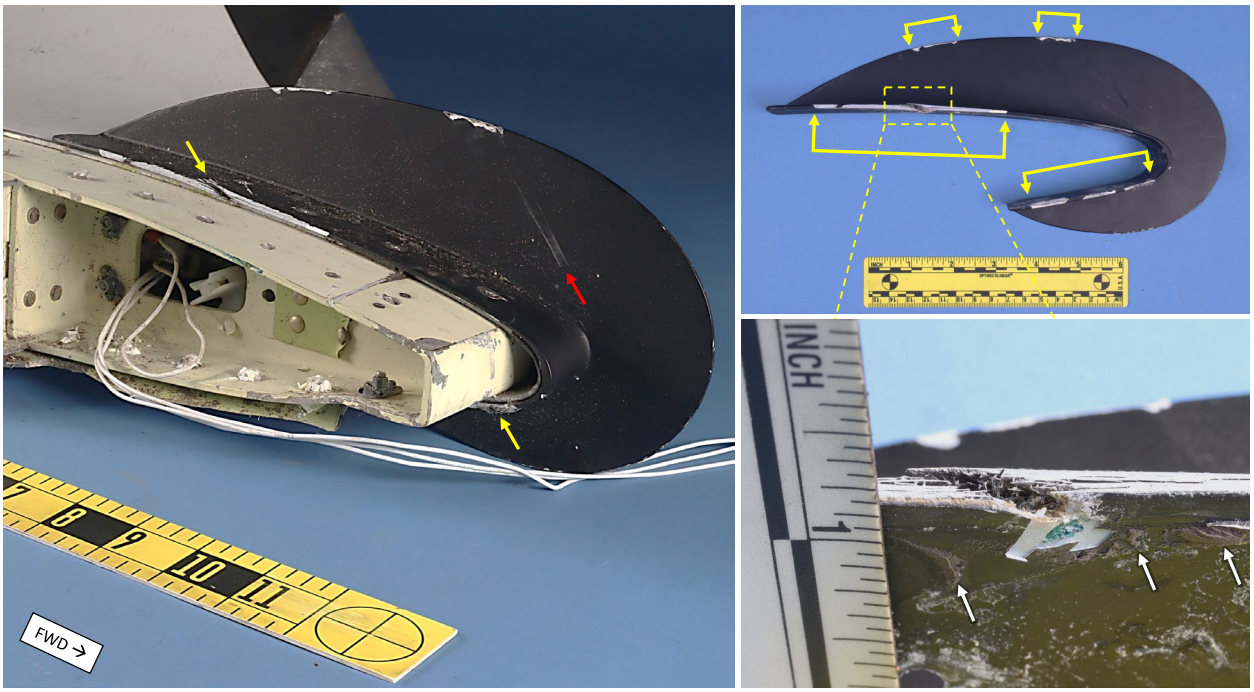

Figure 7. Photograph of the glare shield looking outboard (left) as received with crushed fiber damage indicated by yellow arrows and a witness mark indicated by a red arrow. The upper right image shows the glare shield disassembled with areas of chipped paint indicated by yellow brackets. A closer view of the boxed area is shown in the lower right image where crushed fibers and interlaminar cracks were observed at the inboard edge of the glare shield, and fractured sealant material (white arrows) was observed on the adjacent faying surface.

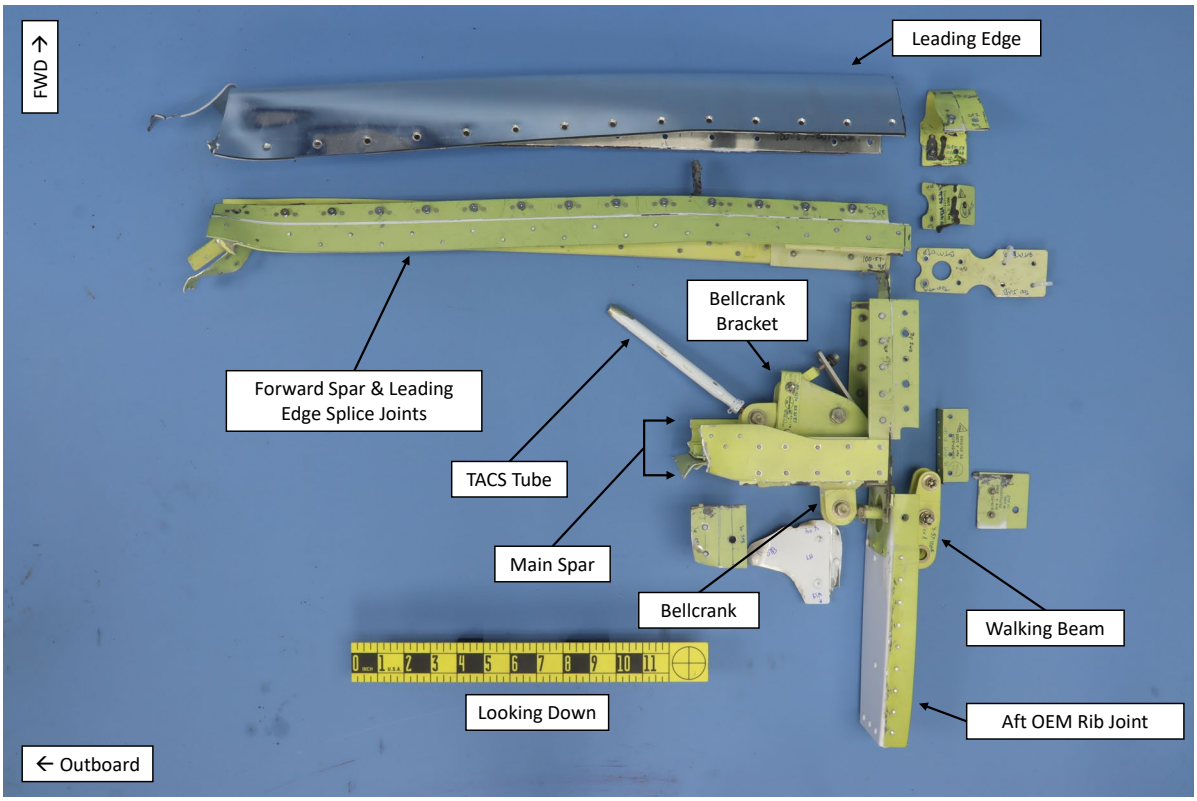

Figure 8. A photograph showing the pieces received from the wing extension assembly.

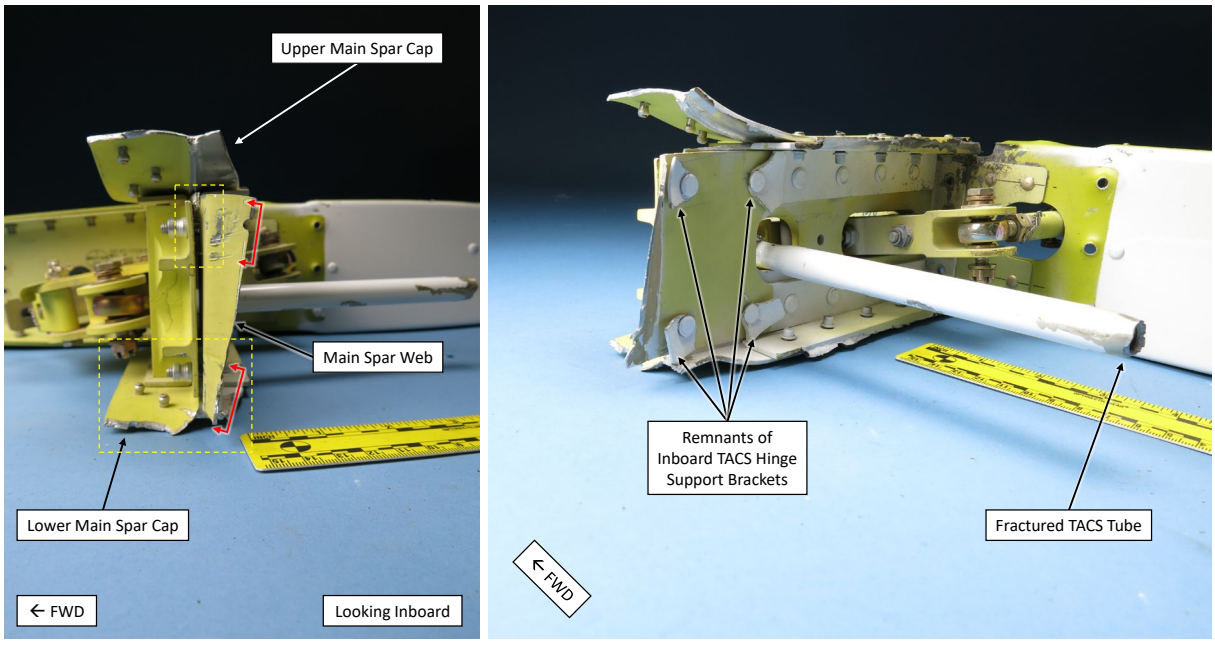

Figure 9. Photographs of the wing extension main spar fracture (inboard location) showing witness marks highlighted by red brackets in the left image. Areas within the yellow boxes are shown more closely in the following figure. The right image indicates portions of the retained TACS hinge support brackets on the aft side of the main spar web and the fractured end of the TACS tube.

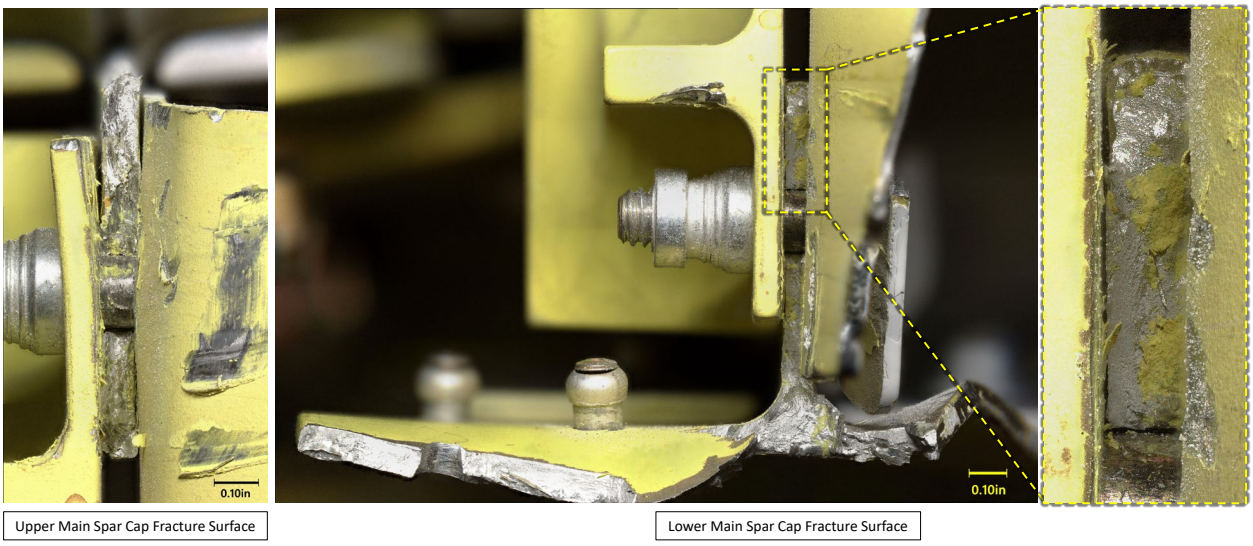

Figure 10. Digital microscope images of the upper (left) and lower (right) fractured main spar caps (inboard location).

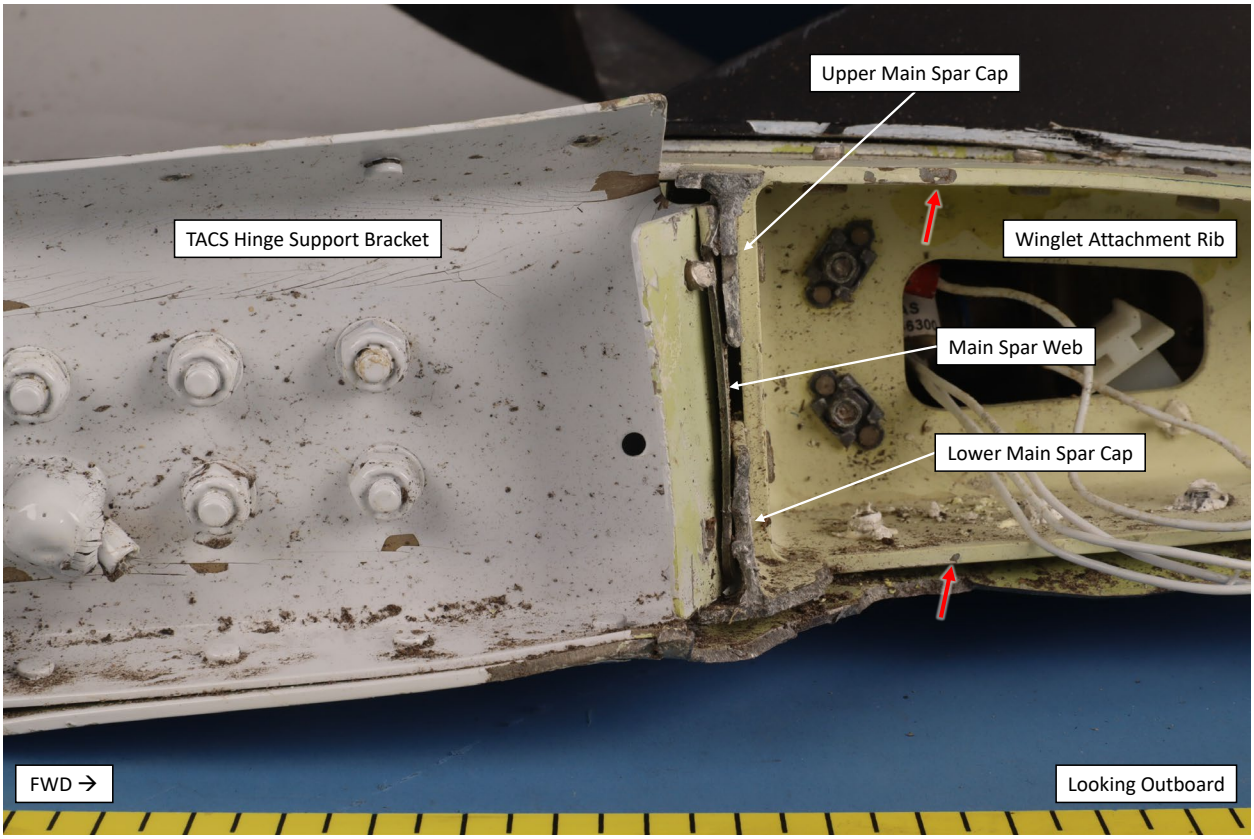

Figure 11. Photograph of the wing extension main spar fracture (outboard location) in the as received condition. Red arrows indicate contact marks on the inboard edges of the winglet attachment rib, forward of the main spar.

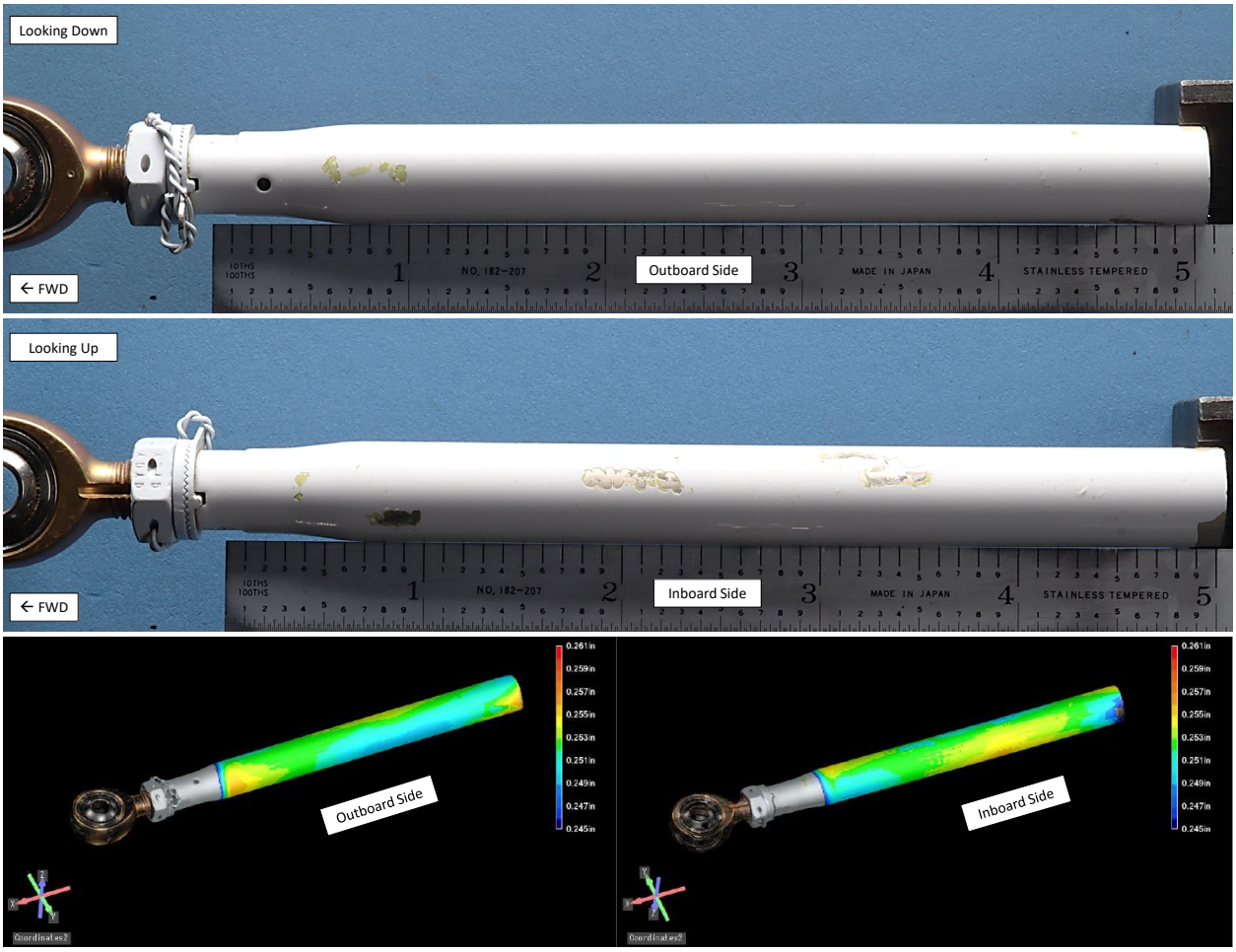

Figure 12. Photographs showing the outboard side (top) and the inboard side (middle) of the TACS tube relative to a straight edge showing small gaps near the center of the outboard side and at each end of the inboard side. Contour maps developed from 3D scanning data displaying variation in tube outer surface radius relative to a best fit cylinder axis are shown at the bottom. Colors at the top of the scale represent larger radii with green representative of nominal radius as calculated from measured diameter using calipers.

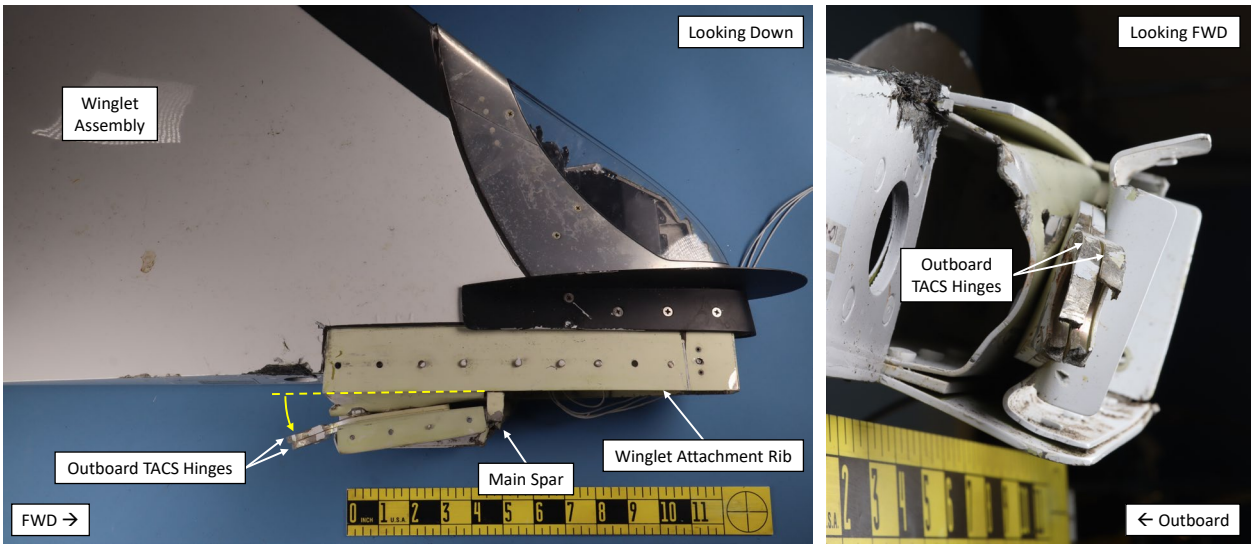

Figure 13. Photographs showing deformation of the outboard TACS hinge brackets as indicated by the yellow dashed line and arrow in the left image.

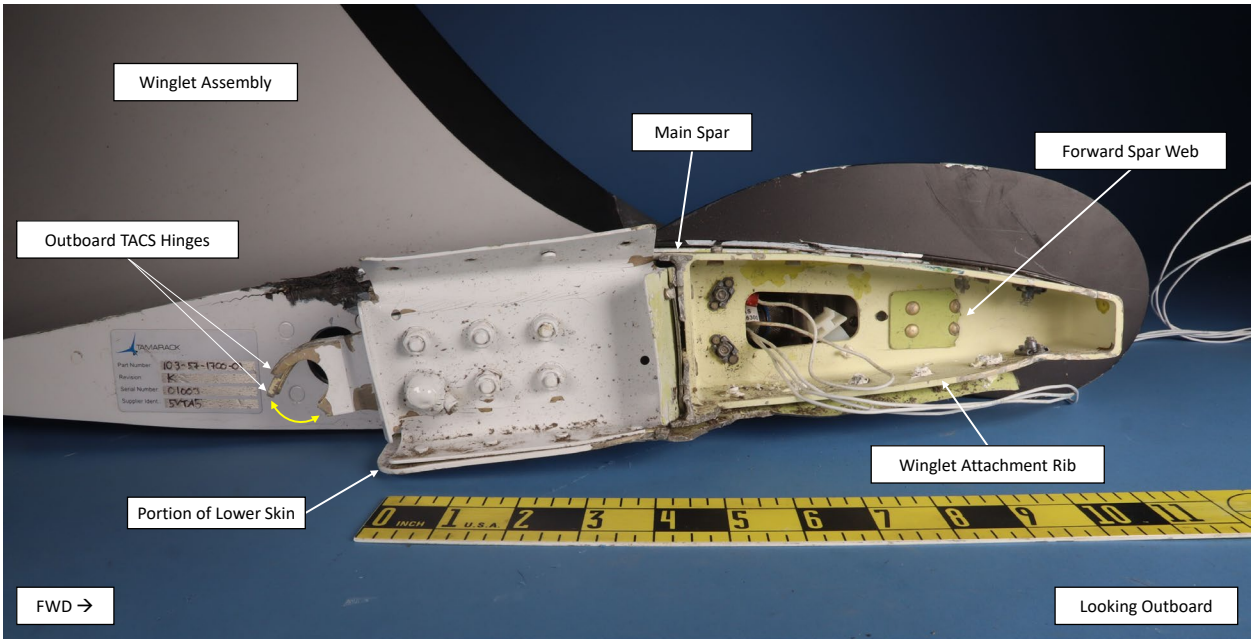

Figure 14. Photograph of the fractured forward spar, main spar (outboard location) and TACS hinge brackets (indicated by the yellow arrow) of the wing extension assembly as viewed looking outboard.

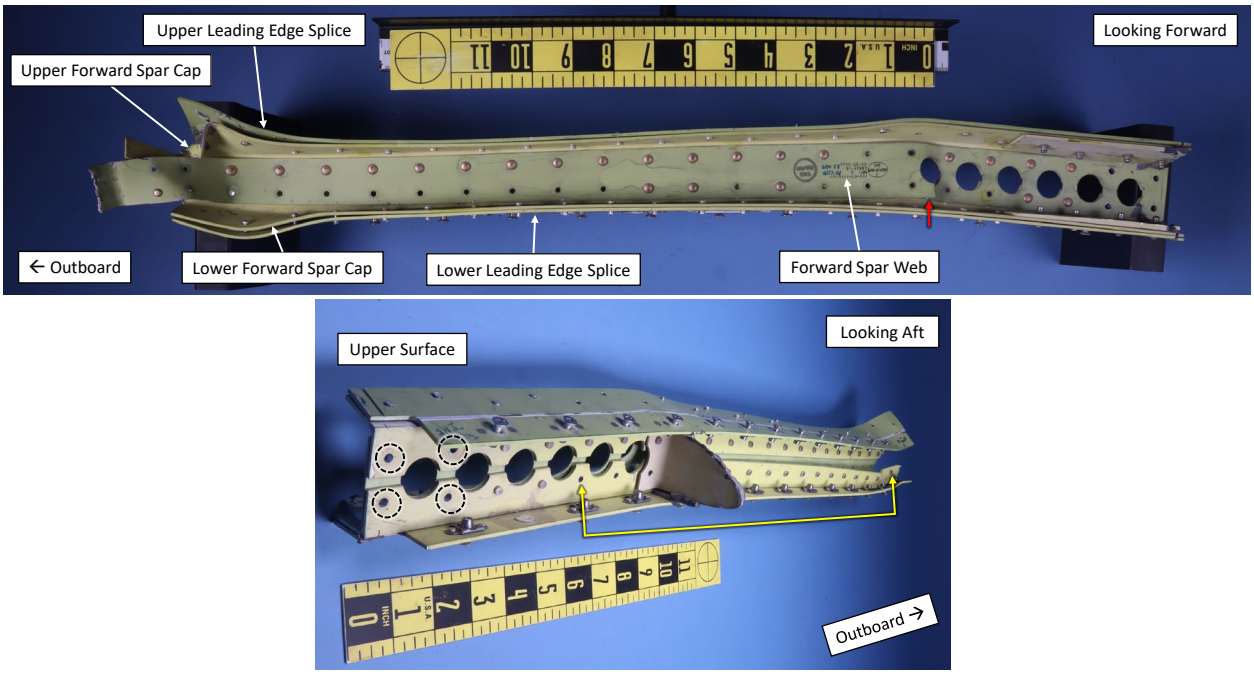

Figure 15. Photographs of the aft side (upper) and forward side (lower) of the wing extension forward spar and leading edge splice joints with the leading edge component removed. The red arrow in the upper image indicates a fracture on the lower side of the forward spar web where localized buckling of the web and upper cap/leading edge splice was observed. The lower image shows fastener separation of the outboard end of the lower forward spar cap from the web indicated by a yellow bracket. The circled locations indicated fasteners removed to aid with disassembly.

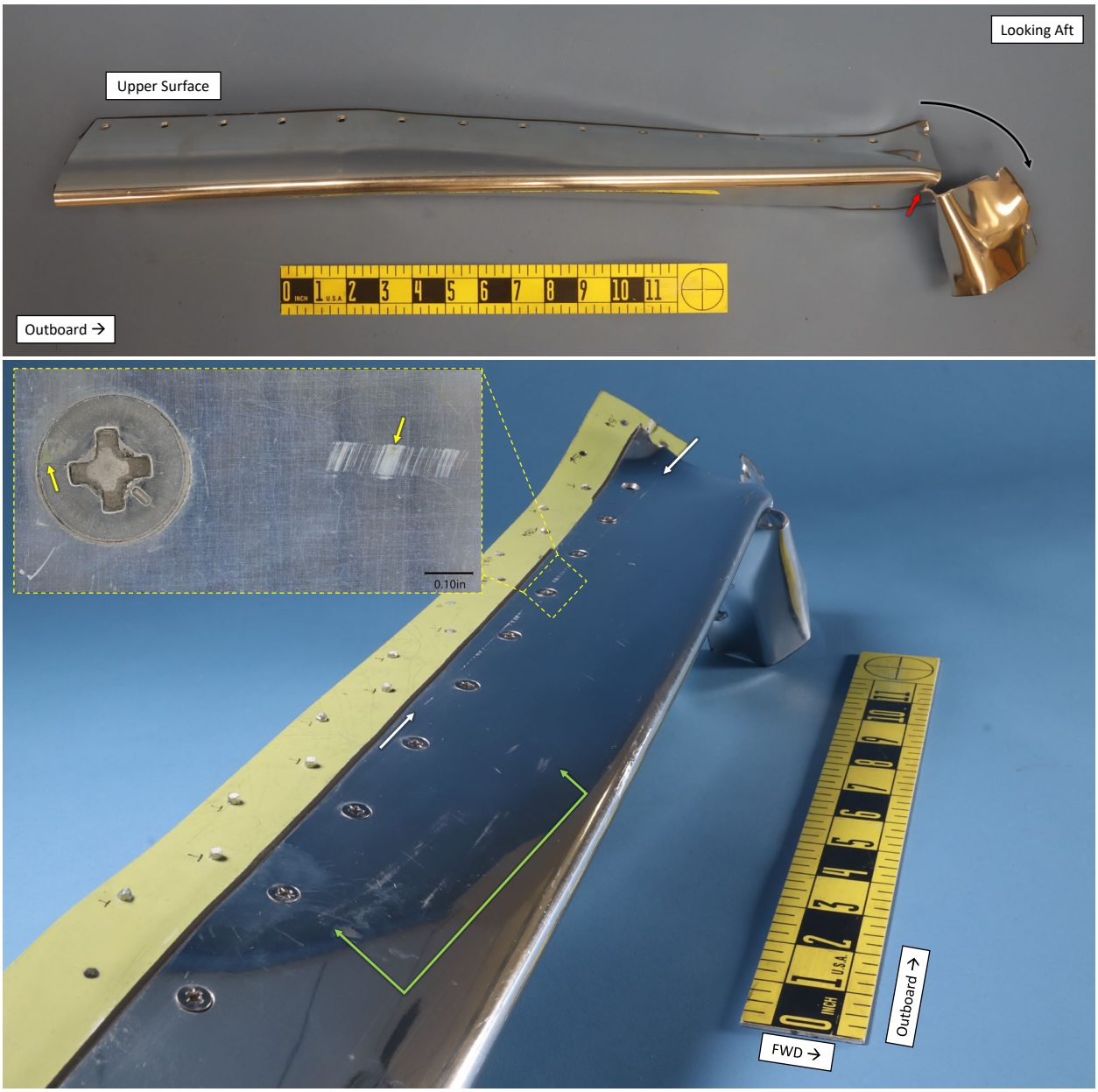

Figure 16. Upper: Photograph of the leading edge component as disassembled from the wing extension assembly showing downward bending (black arrow) near the outboard end from the fracture which arrested on the lower surface near the apex of the leading edge as indicated by the red arrow. Lower: Photograph looking outboard along the leading edge assembled to the forward spar components. A linear streak observed on the upper surface spanned between the two white arrows. A closer view of the boxed area, shown in the inset image shows parallel chordwise scratches and two areas of yellow material transfer indicated by yellow arrows. Abrasions and scratches were also observed in the area indicated by a green bracket.

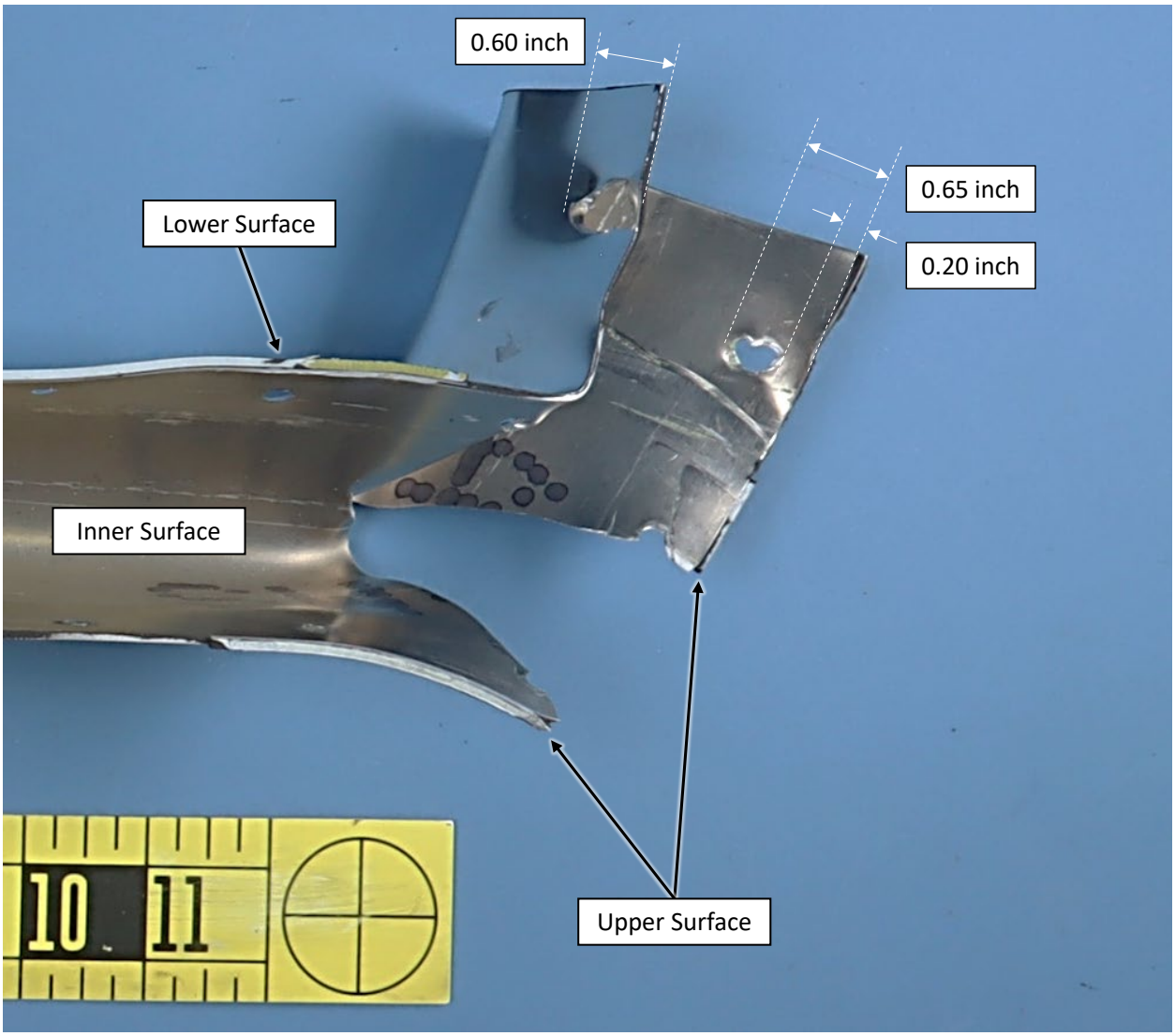

Figure 17. Photograph of the inner surface of the leading edge component showing the elongated outboard fastener hole locations as measured from the aft edge of the part.

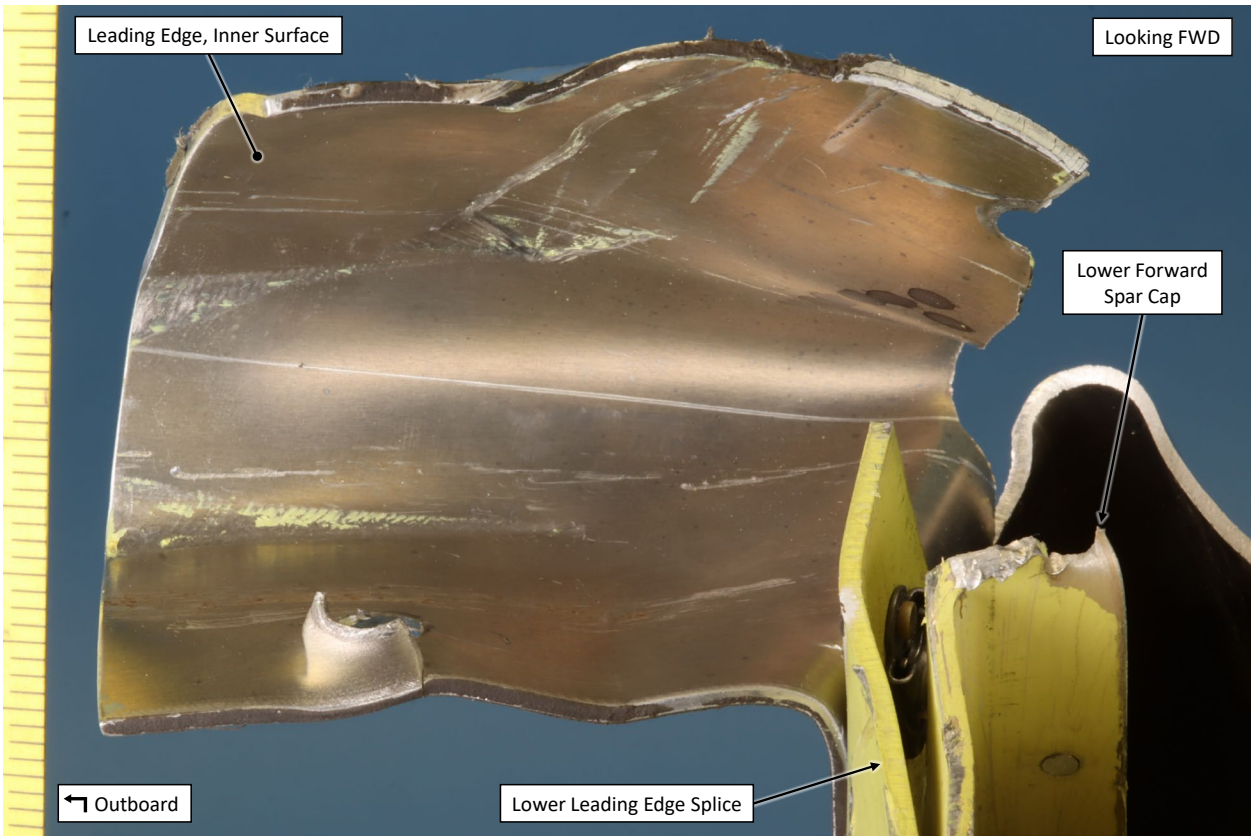

Figure 18. Photograph of the inner surface of the leading edge component after it was reassembled to the leading edge splices. Witness marks such as gouges, dark gray contact marks, and white/yellow paint/primer material transfer was apparent, consistent with contact with the forward end of the winglet attachment rib shown in the following figure.

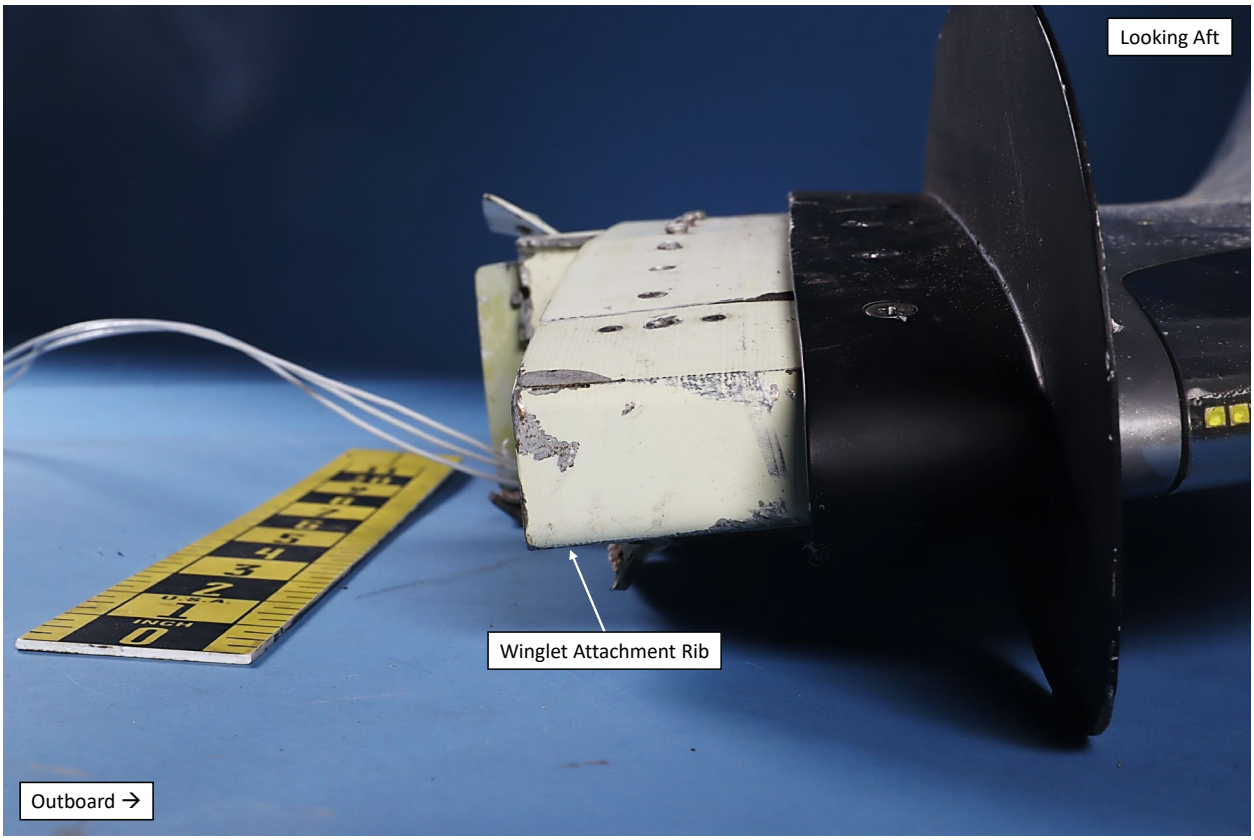

Figure 19. Photograph of the forward end of the winglet attachment rib showing corresponding witness marks (chipped/scraped primer and dark gray contact marks) to the inner surface of the leading edge component.

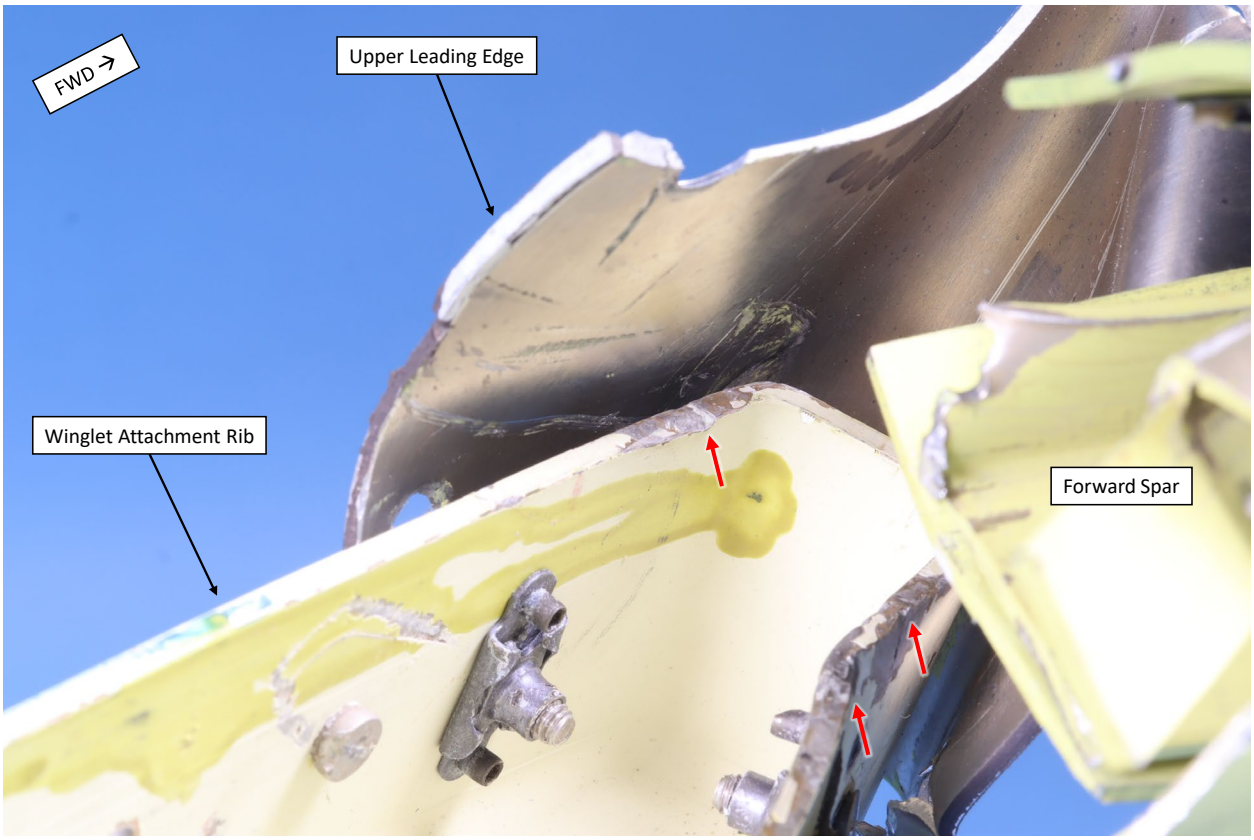

Figure 20. Photograph of the winglet attachment rib placed in close proximity to the connection points on the leading edge component to show the proximity to the witness marks observed on the inner surface of the leading edge. Contact marks on the inboard edge of the winglet attachment rib are indicated by red arrows.

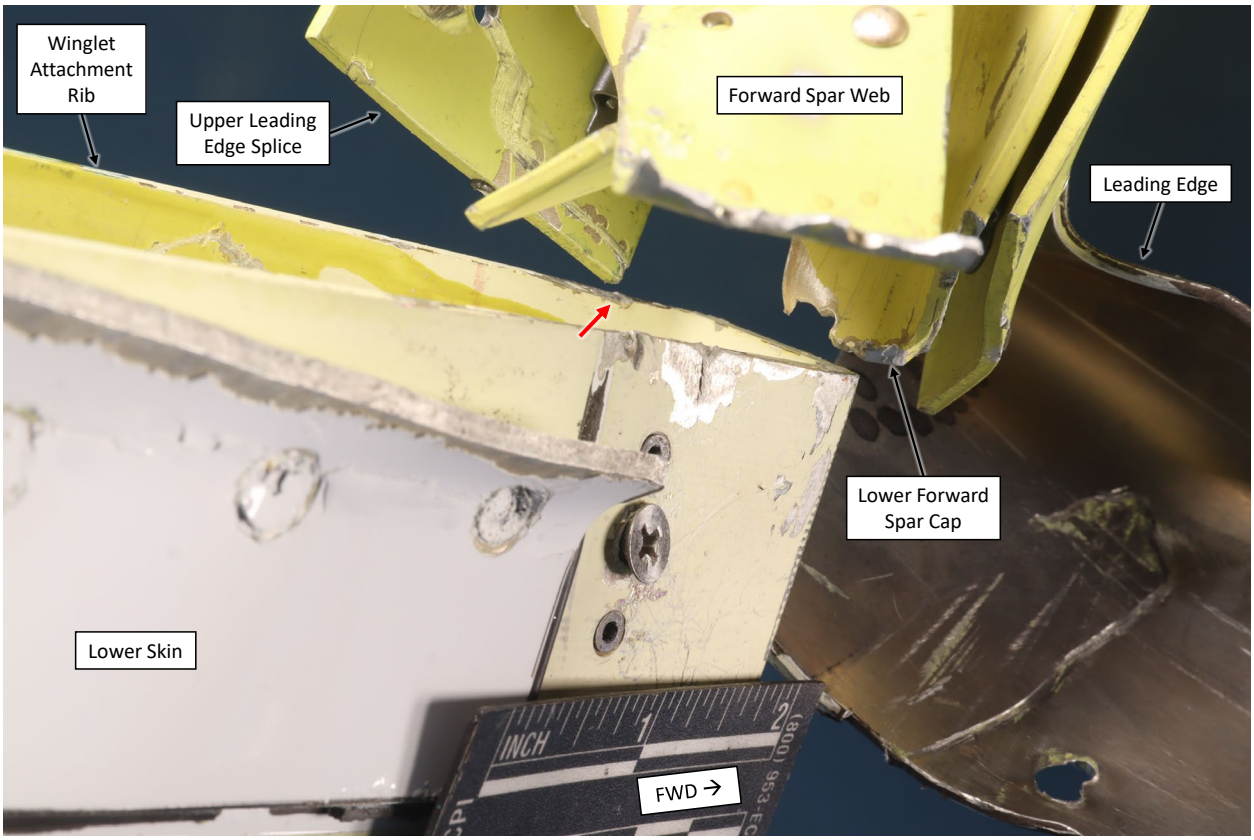

Figure 21. Photograph of the outboard end of the upper leading edge splice aligned with the contact mark on the winglet attachment rib identified in the previous figure (red arrow). The fractured end of the lower forward spar cap closely matches the position of the lower edge of the winglet attachment rib. Scraped and chipped primer was also observed on the lower surface of the upper leading edge splice.

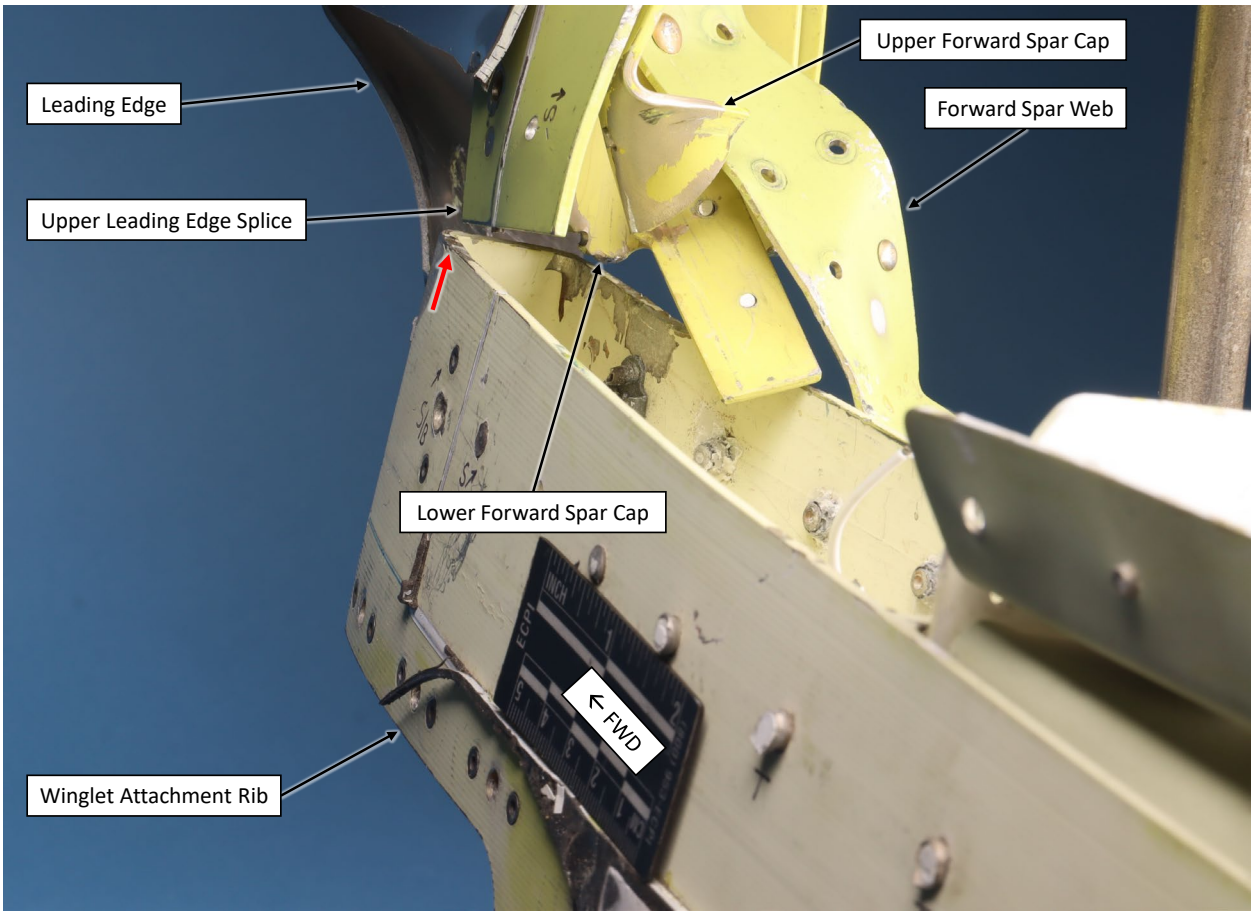

Figure 22. Photograph similar to the previous figure taken from the upper surface. Contact marks and deformation were observed on the upper surface of the upper forward spar cap.

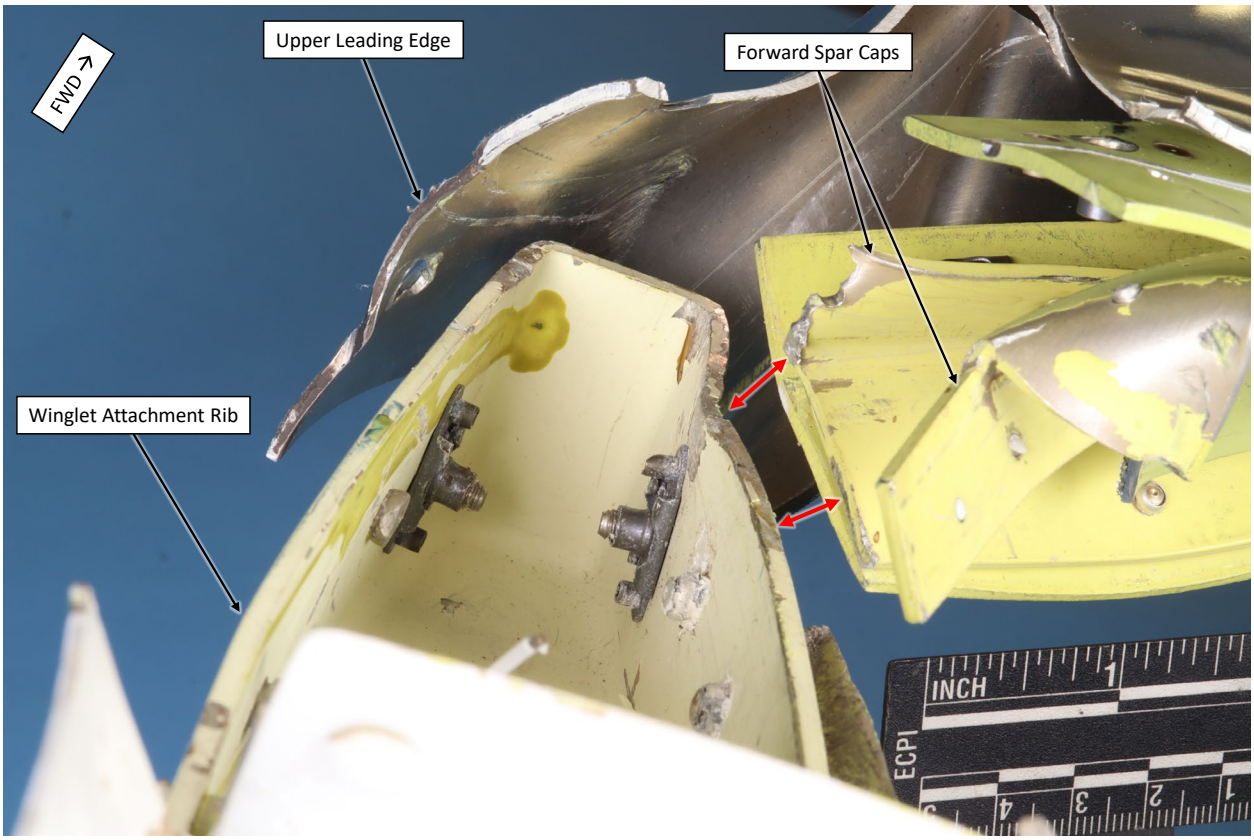

Figure 23. Photograph of the winglet attachment rib aligned with the outboard contact mark on the inner upper surface of the leading edge. Contact marks and deformation observed on the lower inboard edge of the attachment rib corresponded with contact marks observed on the outboard end of the lower forward spar cap as indicated by red arrows. Note the outboard section of the deformed forward spar has been removed for clarity.

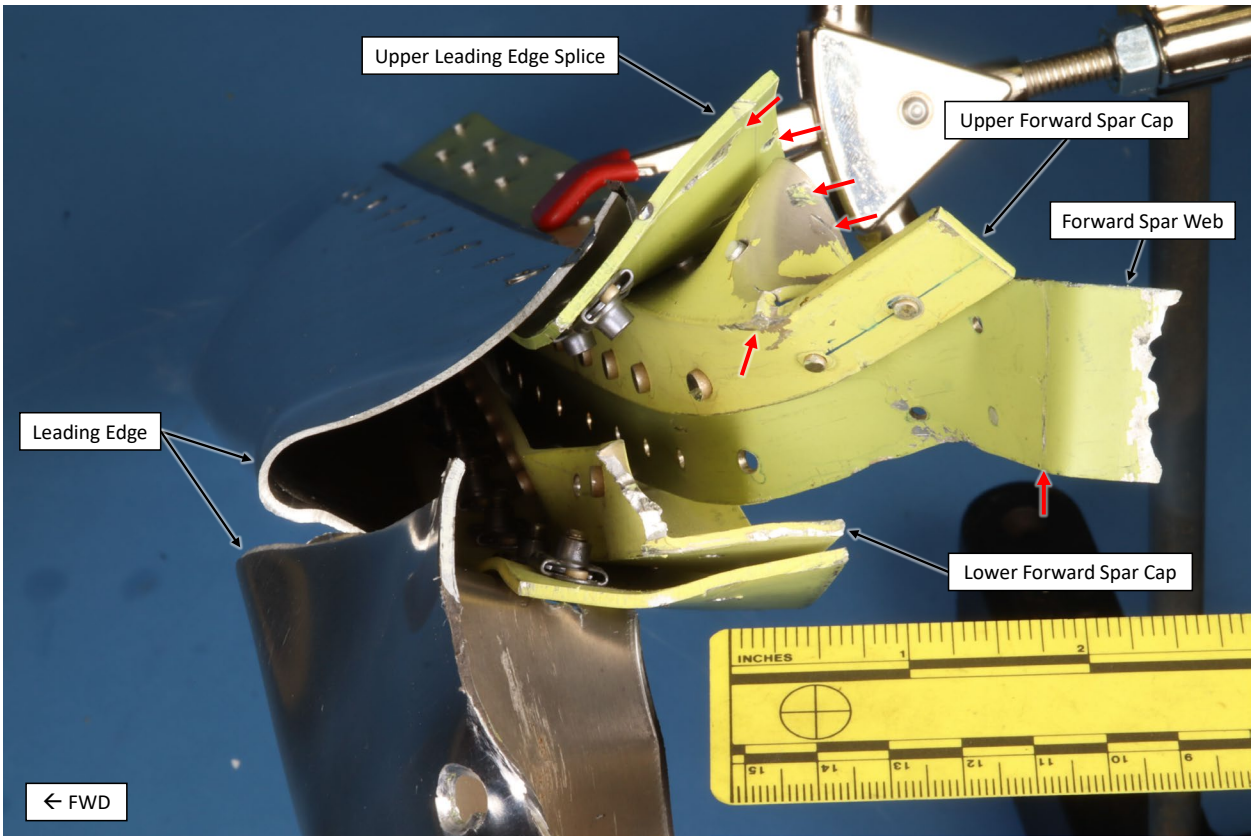

Figure 24. Photograph looking inboard along the forward spar assembled to the leading edge component showing deformation and witness marks (red arrows) near the outboard end. The lower spar cap was separated along the fastener row which connected to the web.

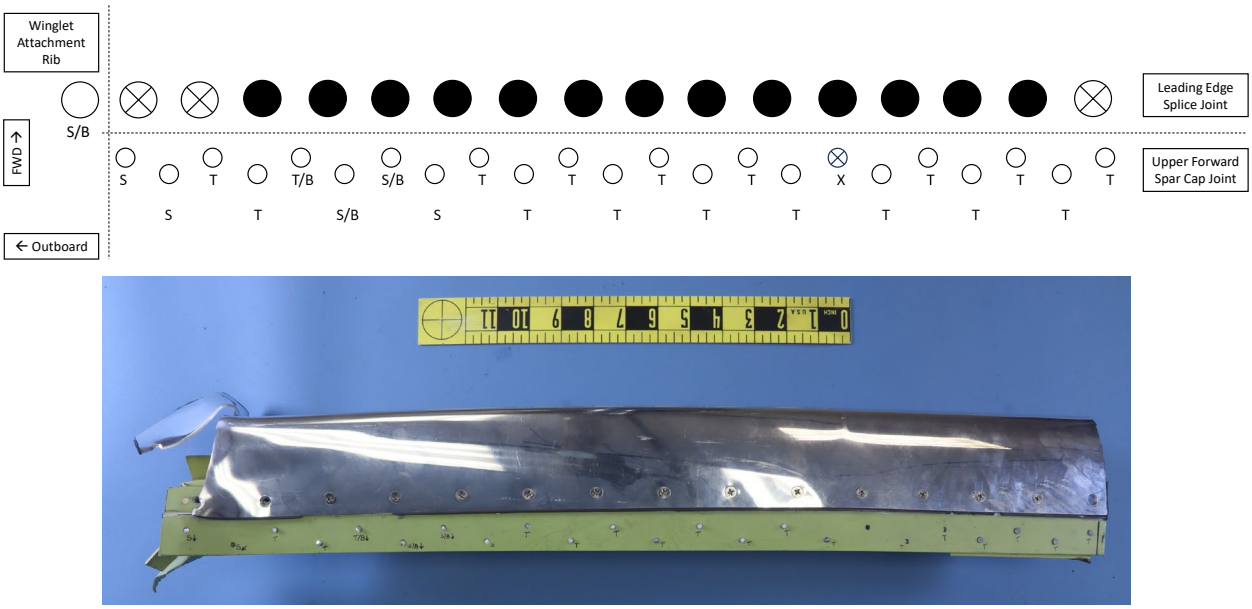

Figure 25. Schematic of the upper leading edge splice joint and upper skin-to-forward spar fastener conditions along the wing extension. Fractured fasteners are identified by an open circle, missing fasteners by a circle with an "X" and intact fasteners by a filled circle. Fracture designations are T = tensile fracture mode, S = shear fracture mode, B = mixed mode bending fracture used in conjunction with T or S as applicable.

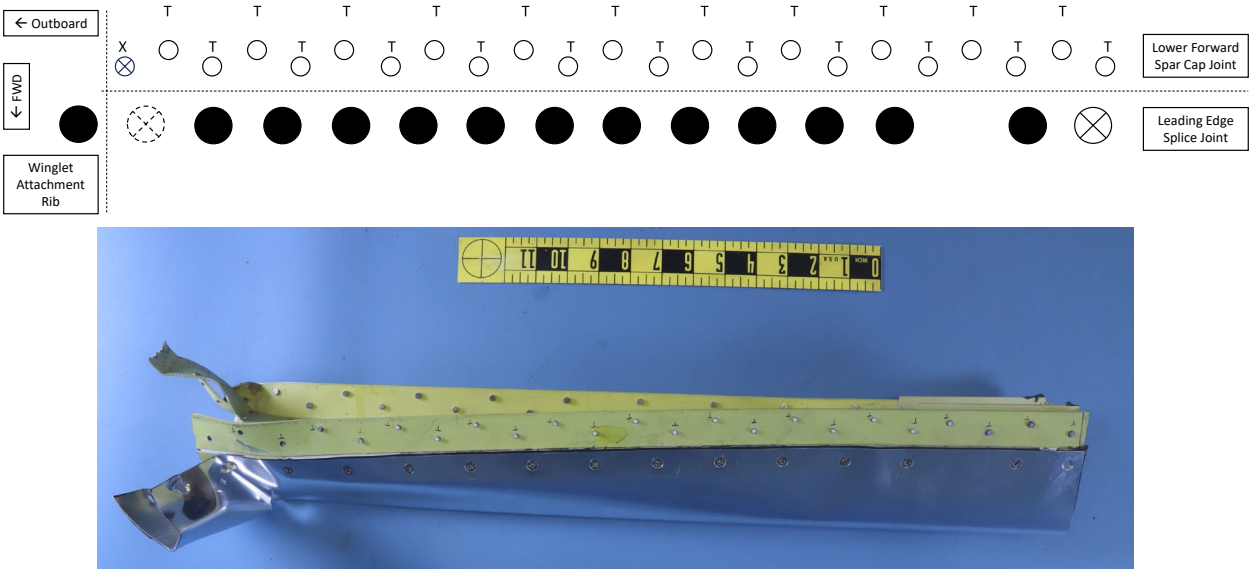

Figure 26. Schematic of the lower leading edge splice joint and lower skin-to-forward spar fastener conditions along the wing extension. Fractured fasteners are identified by an open circle, missing fasteners by a circle with an "X" and intact fasteners by a filled circle. Fracture designations are T = tensile fracture mode, S = shear fracture mode, B = mixed mode bending fracture used in conjunction with T or S as applicable. The fastener represented by a dashed "X" circle was drilled out to aid with disassembly.

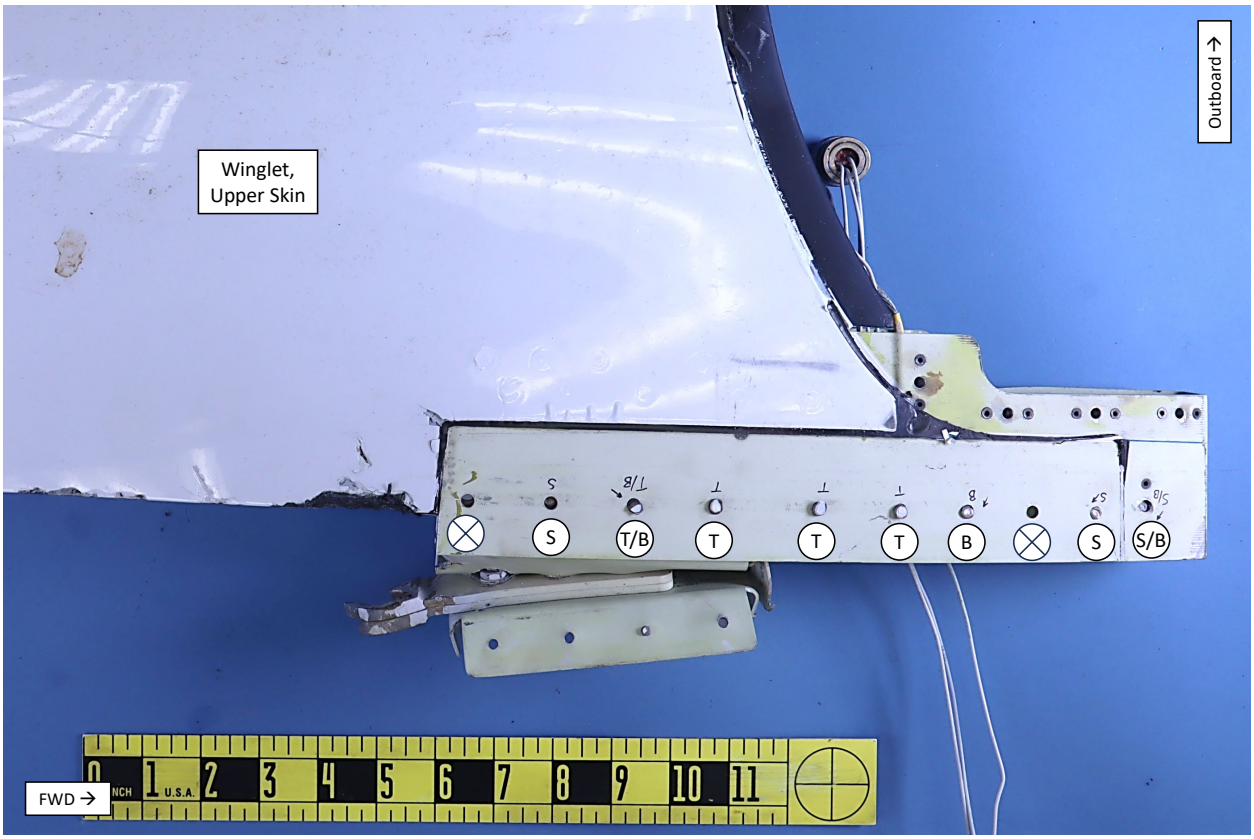

Figure 27. Schematic of the wing extension upper skin-to-winglet attachment rib fastener conditions. Fractured fasteners are identified by an open circle, missing fasteners by a circle with an "X" and intact fasteners by a filled circle. Fracture designations are T = tensile fracture mode, S = shear fracture mode, B = mixed mode bending fracture used in conjunction with T or S as applicable.

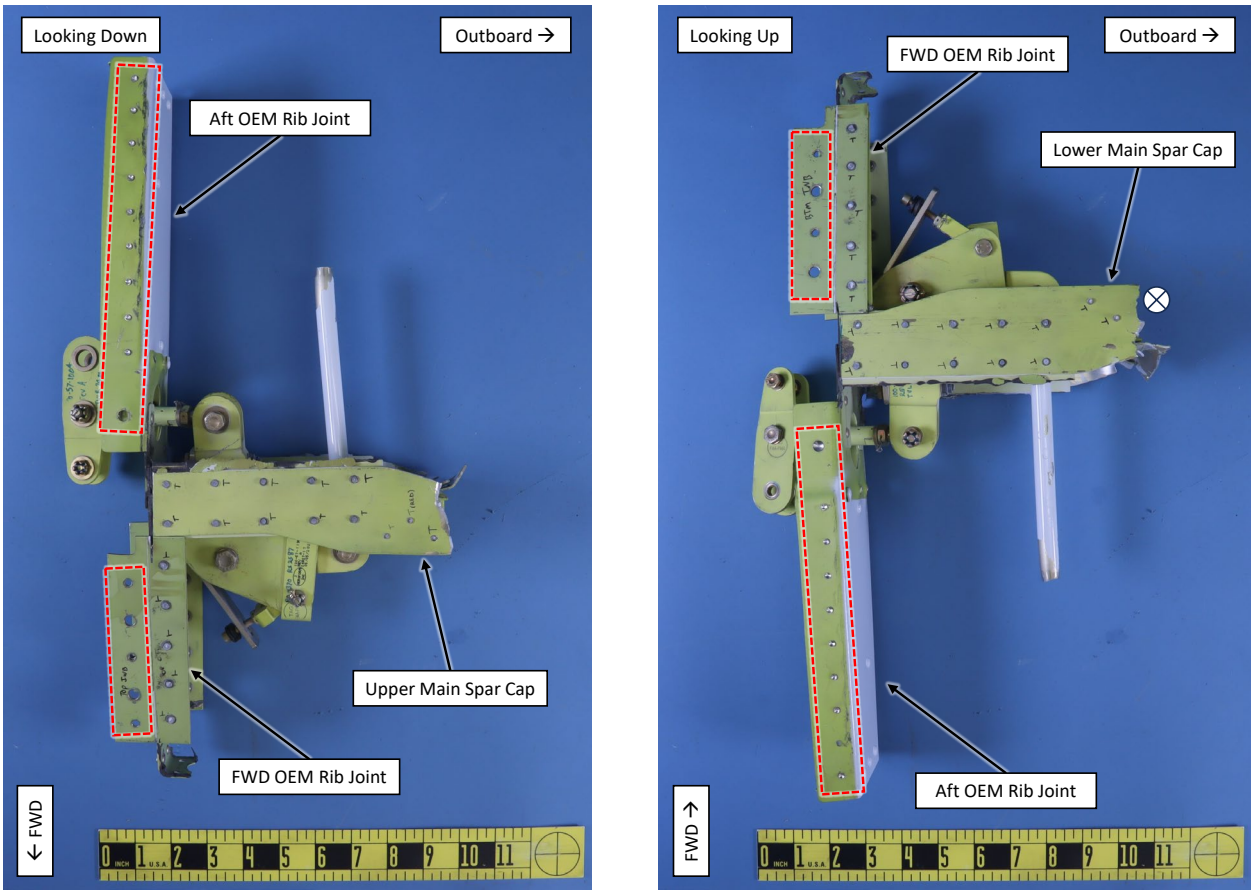

Figure 28. Schematic of the inboard wing extension upper skin (left) and lower skin (right) fastener conditions. All fractured fasteners exhibited tensile fracture modes. Fastener locations within the red boxes were drilled out to aid with disassembly from the accident airplane.

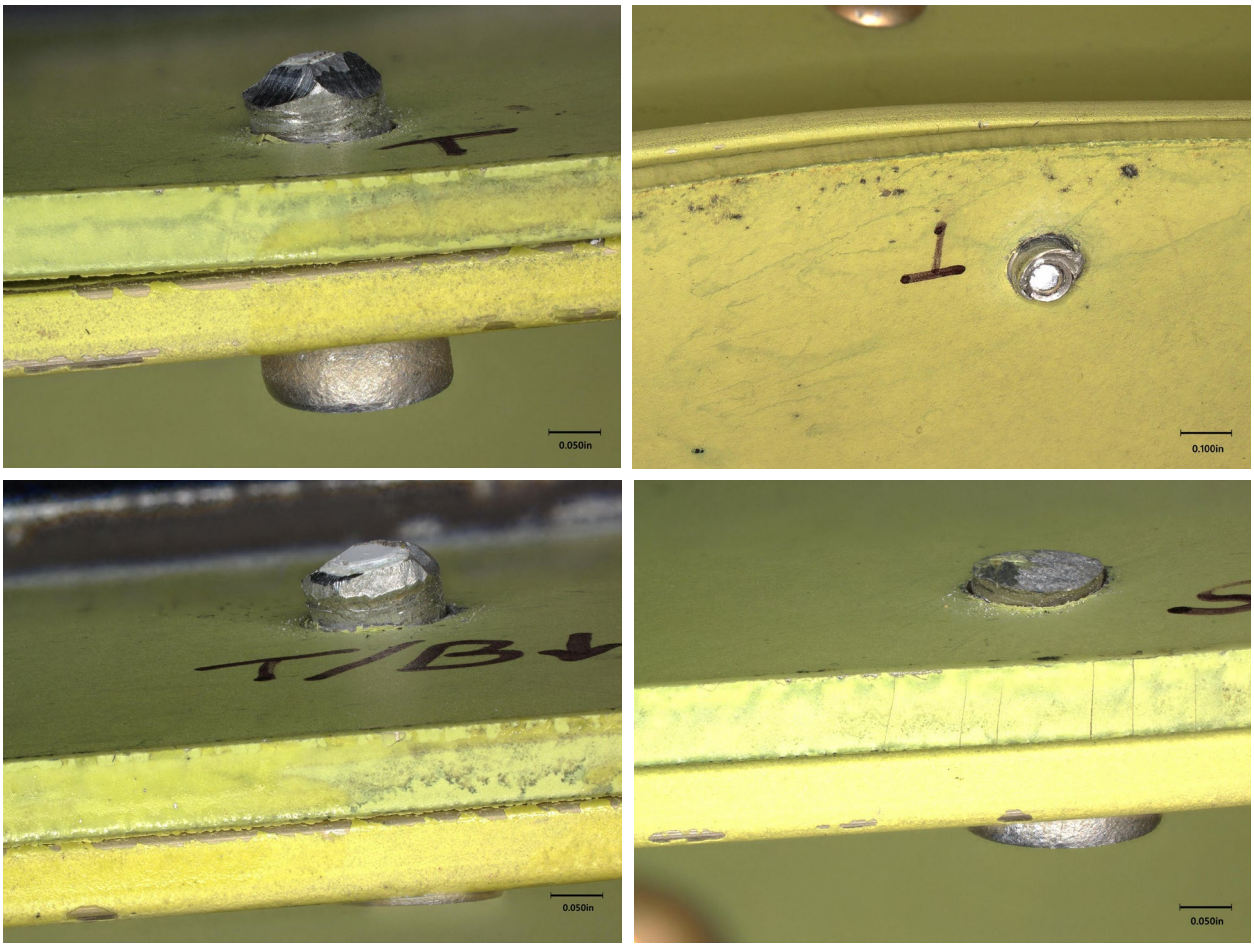

Figure 29. Digital microscope images showing typical fractured fastener characteristics for solid rivet tensile fracture mode (upper left), solid rivet tensile/bending fracture mode (lower left), blind rivet tensile fracture mode (upper right), and solid rivet shear fracture mode (lower right).

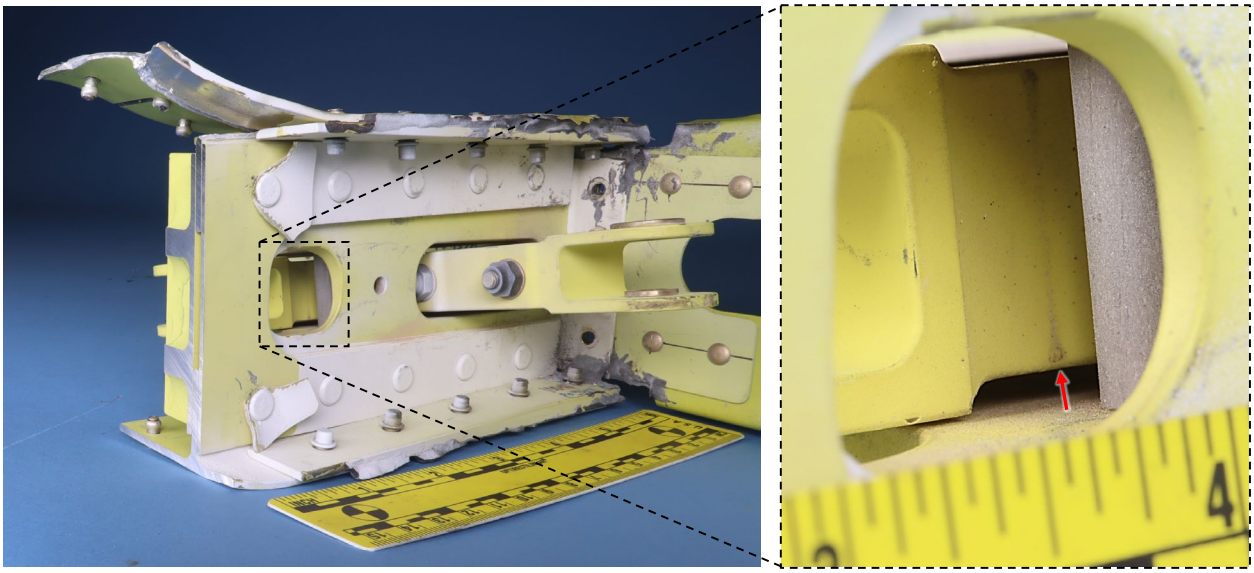

Figure 30. Photograph of the aft side of the bellcrank mechanism showing a light contact mark indicated by a red arrow in the right image which closely matched the position of the forward side of a bushing on the bellcrank bracket.

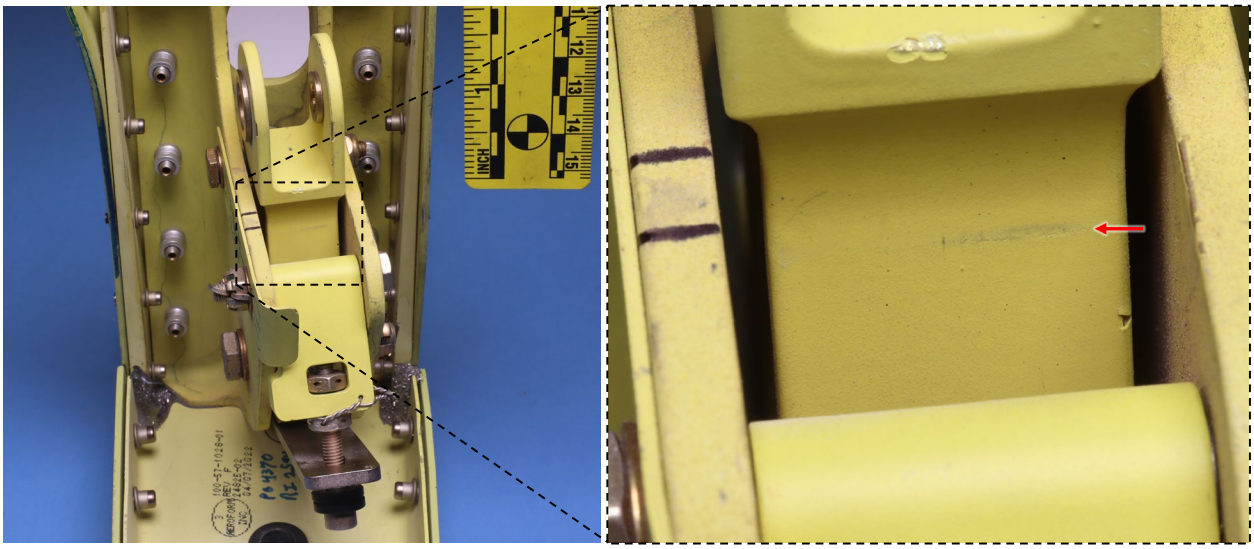

Figure 31. Photograph of the forward side of the bellcrank mechanism showing a light contact mark indicated by a red arrow in the right image which closely matched the position of the TACS return bracket.

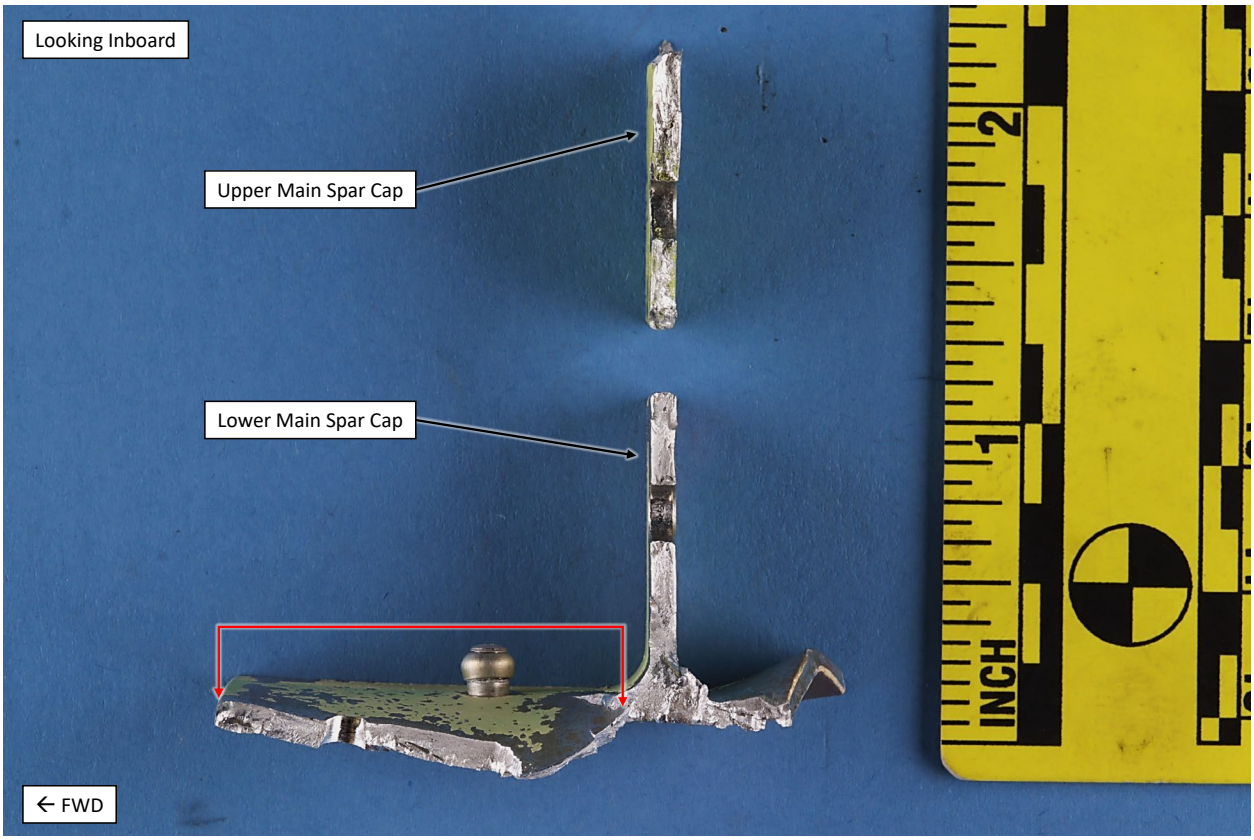

Figure 32. Photograph of the main spar cap fracture surfaces (inboard fracture location) showing a secondary crack along the forward flange of the lower main spar cap indicated by the red bracket. Bending and buckling deformation was observed along the lower flanges. Smearing and contact damage was observed on the upper spar cap fracture surface, around the fastener holes, and along the aft flange fracture surface.

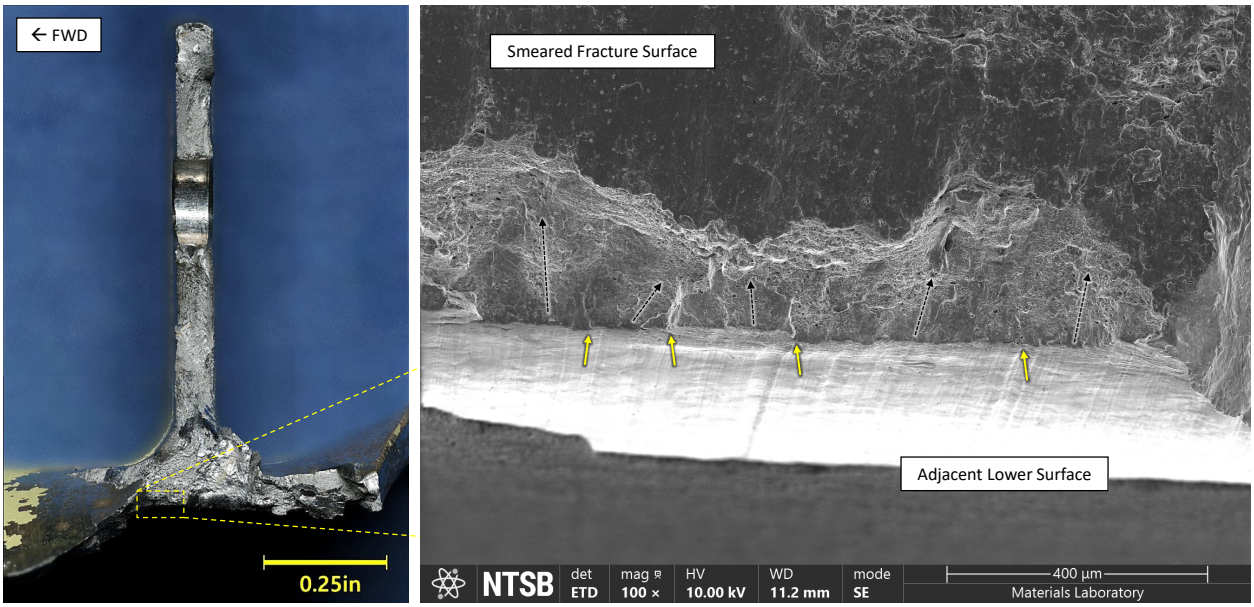

Figure 33. Secondary electron fractograph (right) of the lower main spar cap fracture and adjacent lower surface in the area indicated by the yellow box in the left image. Fracture initiation sites (yellow arrows) were observed emanating from the lower surface from parallel features consistent with machining marks or extrusion lines observed on the lower surface. The fracture progressed over a relatively flat plane as indicated by black arrows before transitioning to rougher fracture features that were obscured by smearing damage.

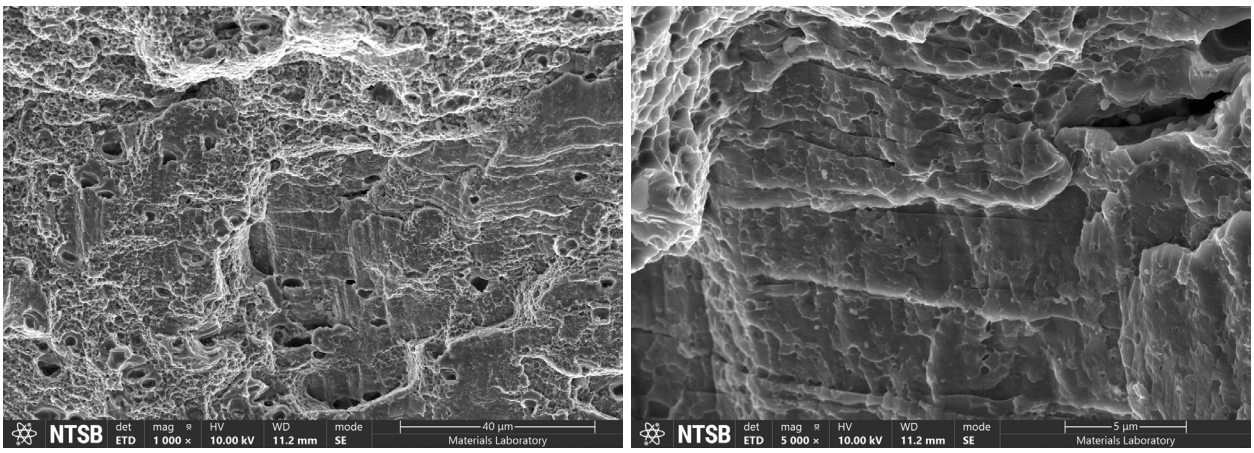

Figure 34. Secondary electron fractographs of the previous figure at higher magnifications showing dimpled features interspersed with islands of striated features oriented horizontally in these images.

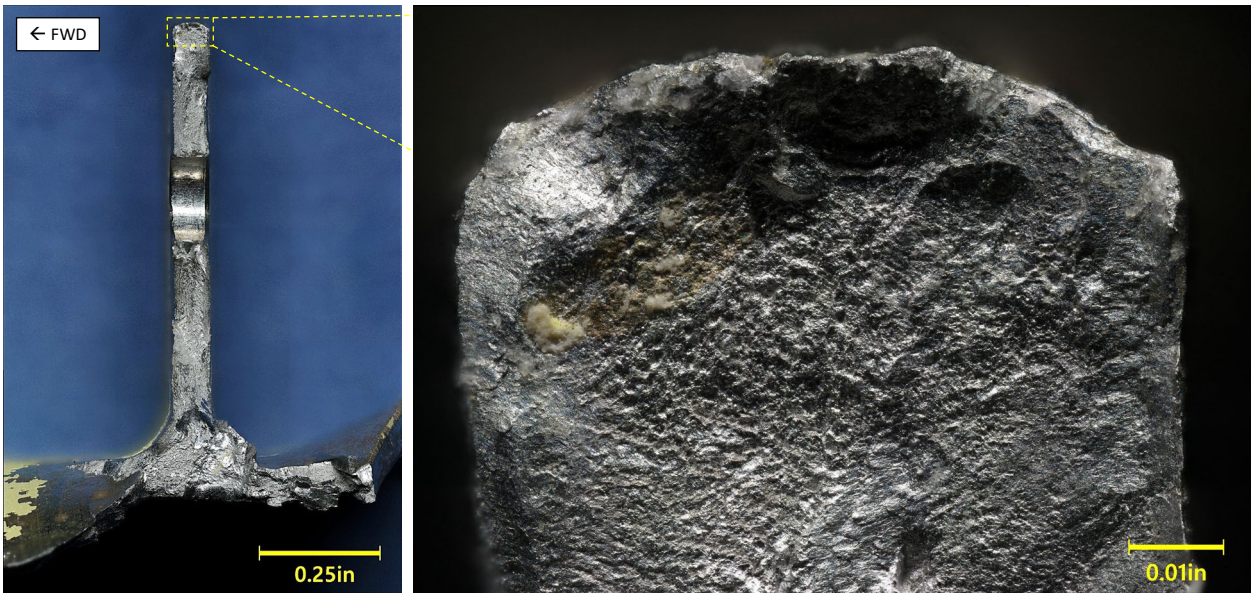

Figure 35. Digital microscope images of the fracture surface near the upper edge of the lower main spar cap (inboard fracture location) showing a smeared and battered appearance consistent with post separation contact damage.

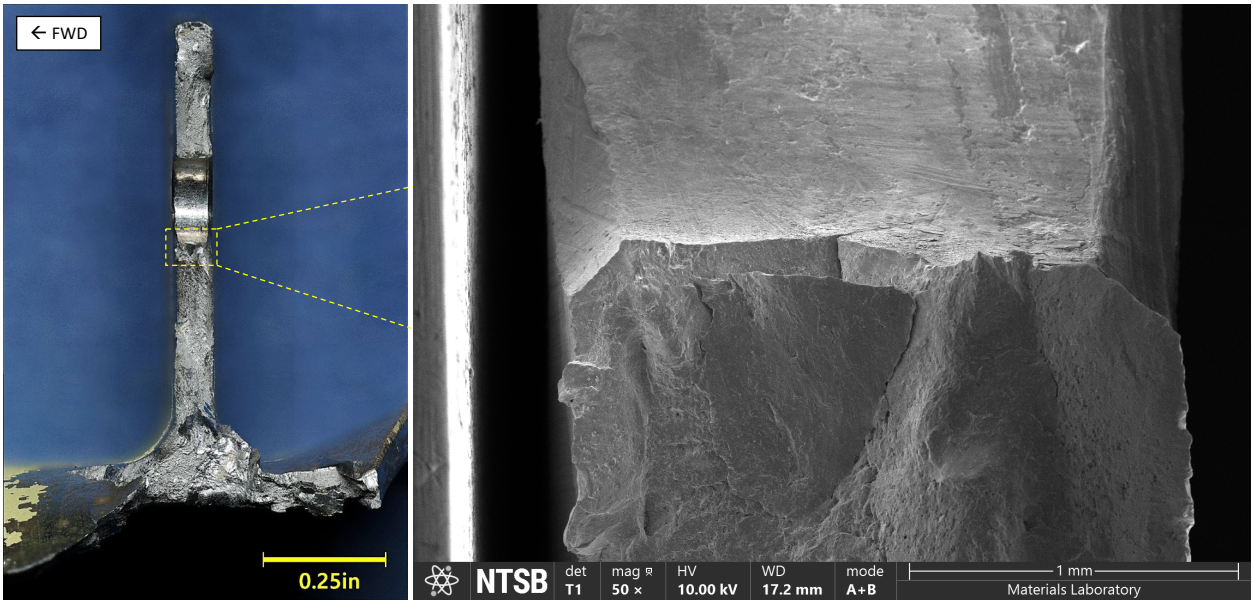

Figure 36. Secondary electron fractograph (right) of the lower main spar cap fracture surface (inboard fracture location) below the fastener hole showing mechanical contact damage.

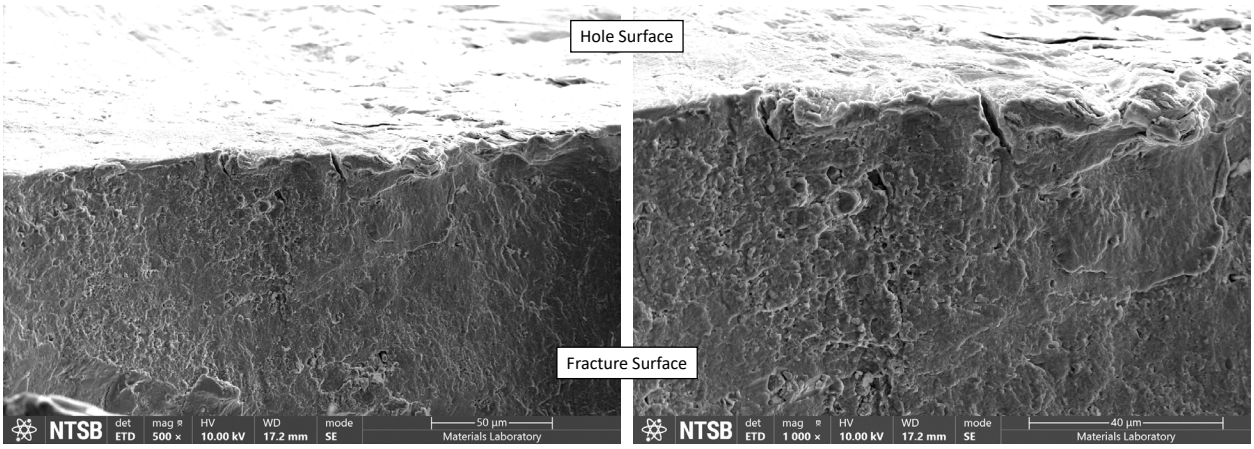

Figure 37. Secondary electron fractographs of the previous figure at higher magnifications showing dimpled fracture features where smearing damage was less pronounced.

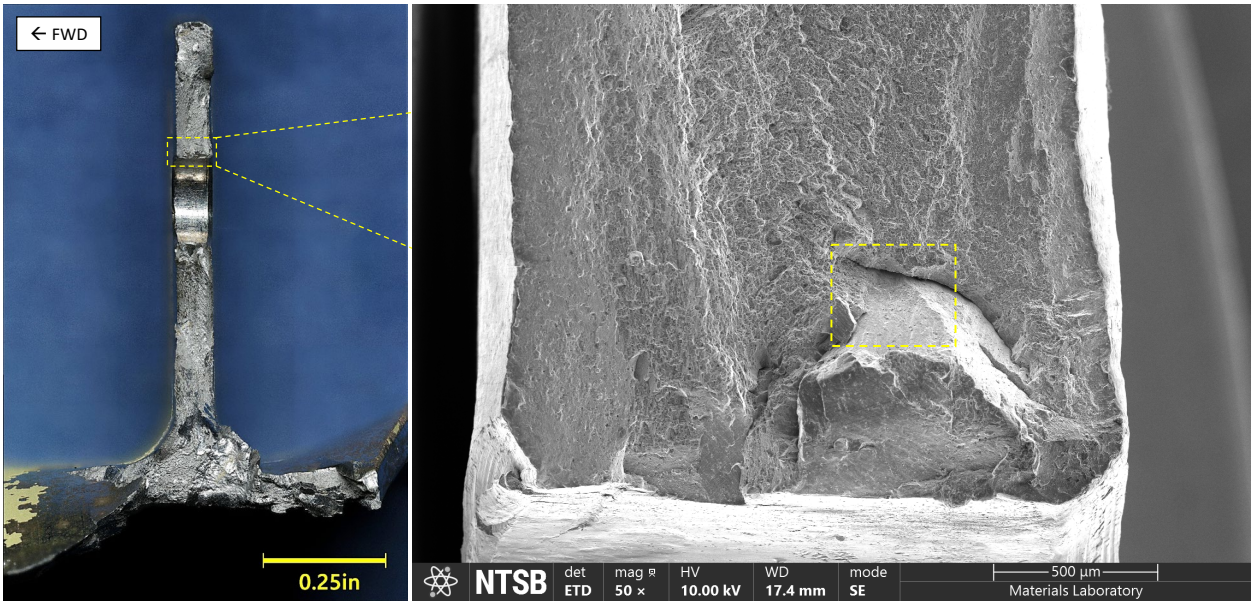

Figure 38. Secondary electron fractograph (right) of the lower main spar cap fracture surface (inboard fracture location) above the fastener hole showing mechanical contact damage. Shear lip features and necking deformation were observed along the forward and aft edges of the stem with a rougher central region between. The area highlighted by a yellow box in the right image was observed more closely as detailed in the following figures.

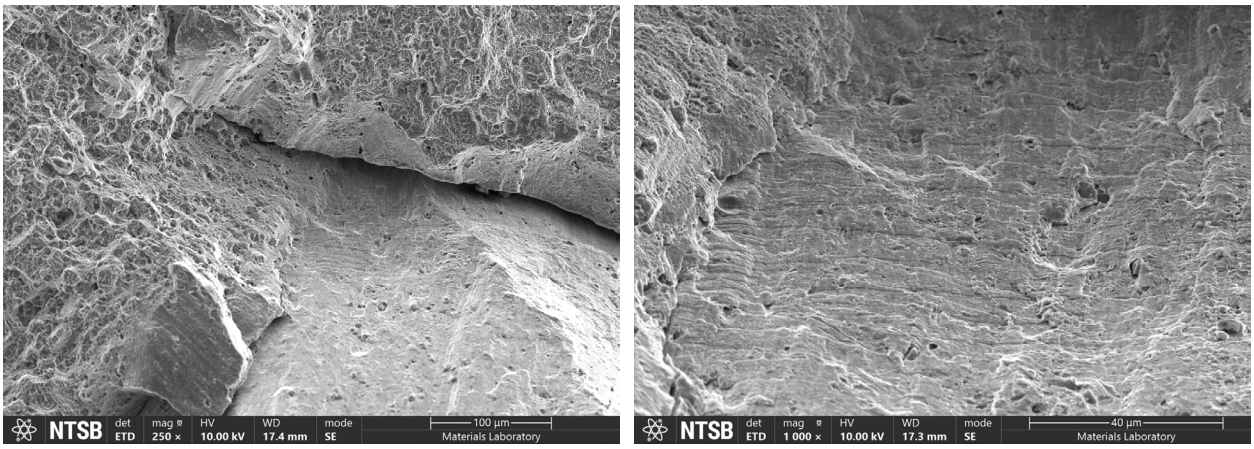

Figure 39. Secondary electron fractographs of the previous figure at higher magnification showing horizontally oriented striated features interspersed with dimpled fracture features.

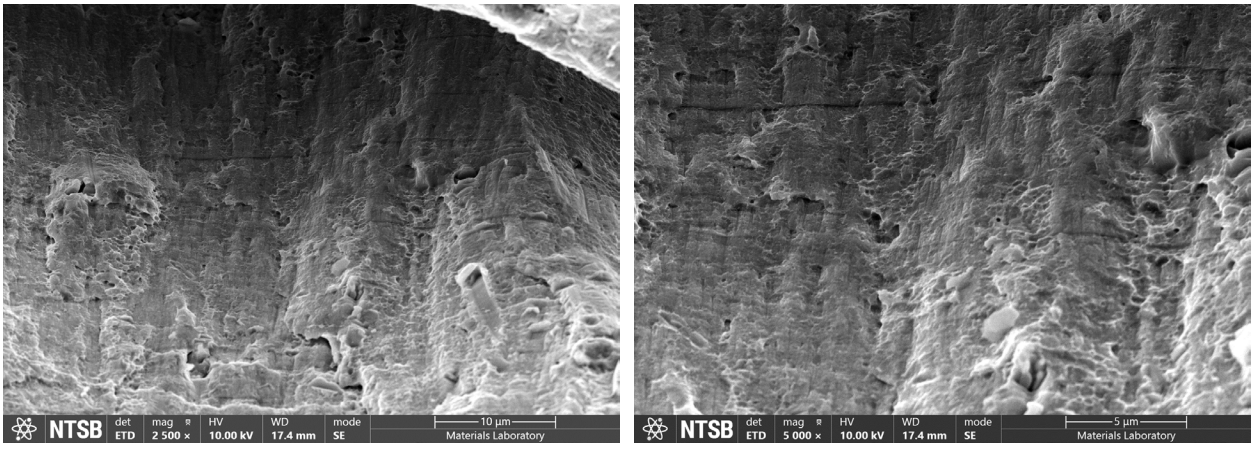

Figure 40. Secondary electron fractographs of the previous figure at higher magnifications.

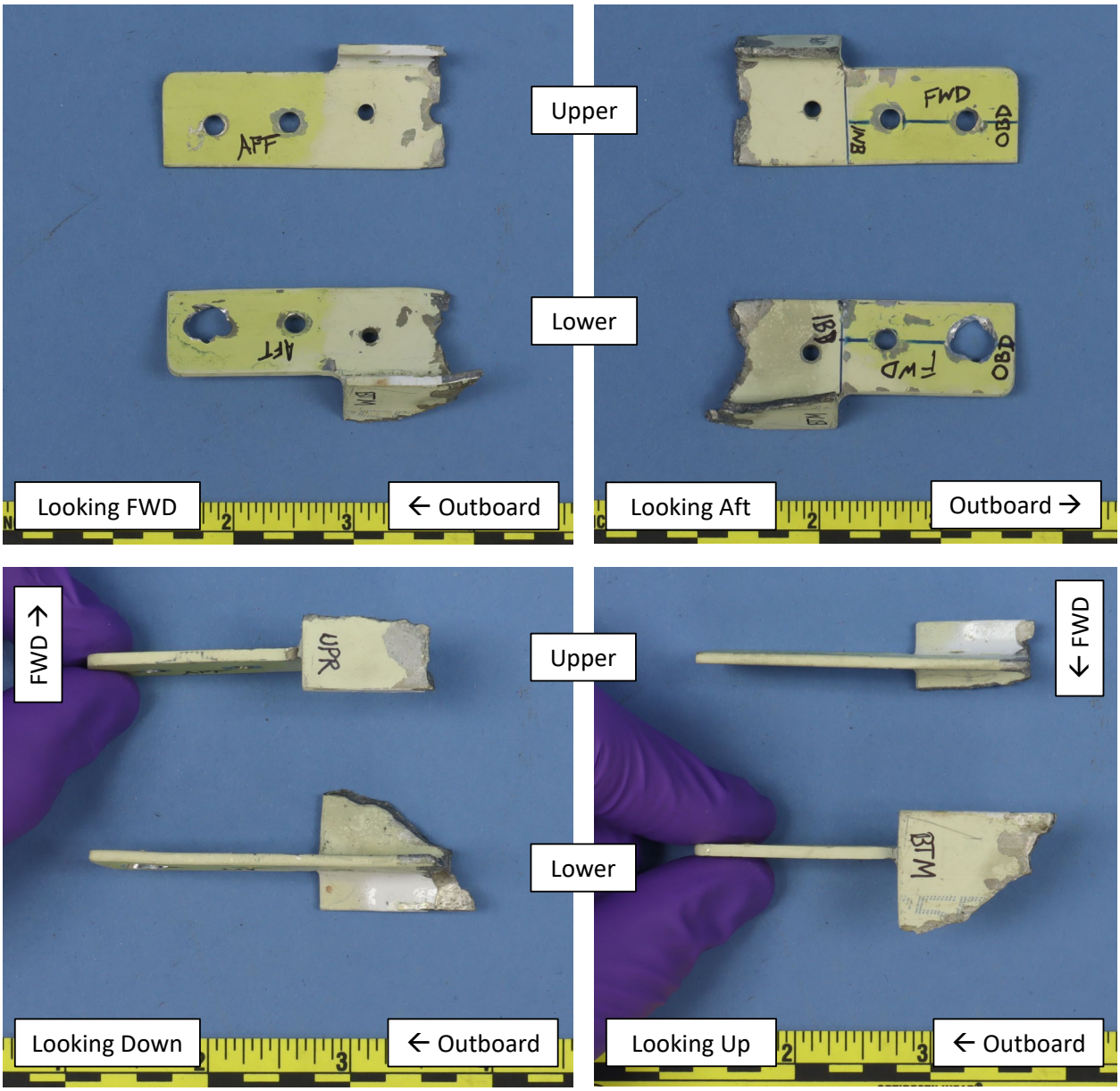

Figure 41. Photographs of the fractured main spar caps (outboard fracture location) after disassembly from the winglet attachment rib, main spar web, and TACS hinge support brackets.

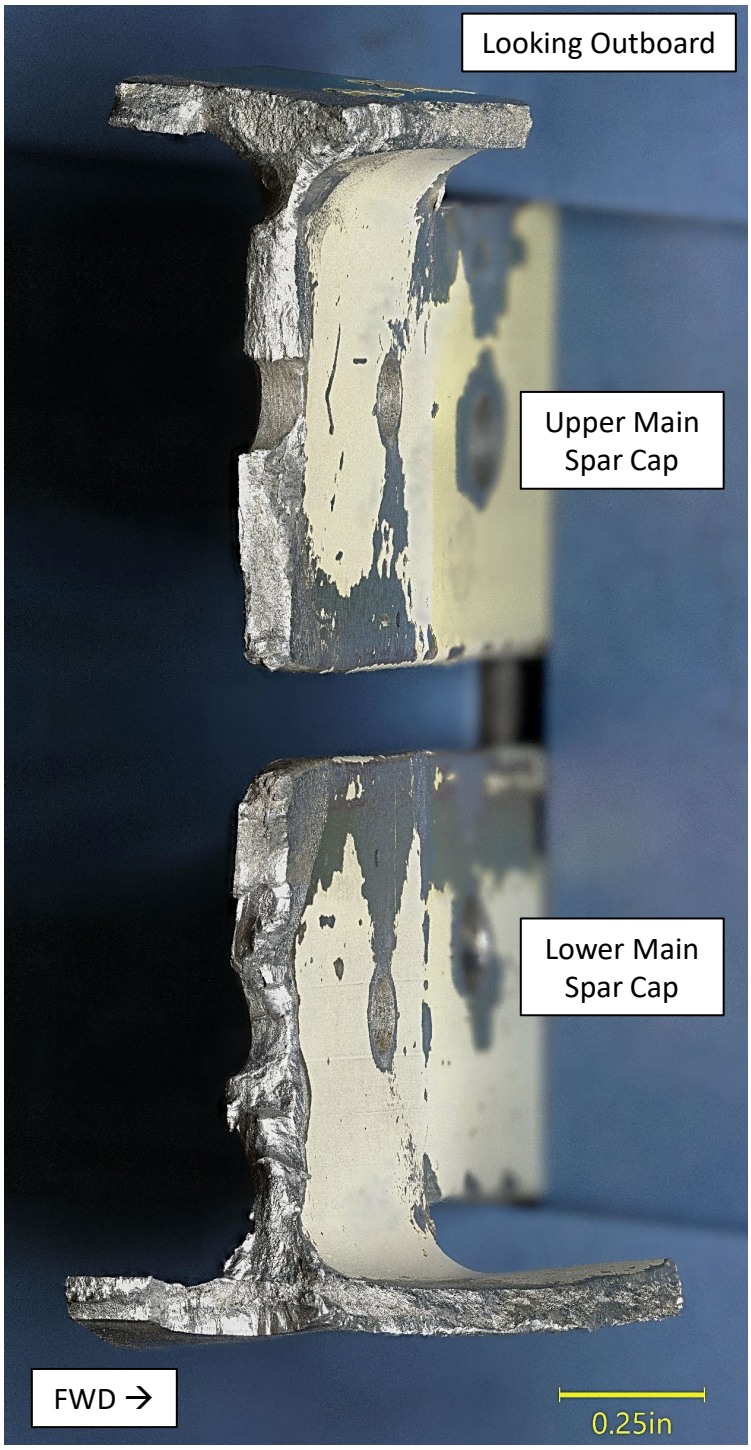

Figure 42. Digital microscope image of the upper and lower main spar cap fracture surfaces (outboard fracture location) viewed tilted slightly aft.

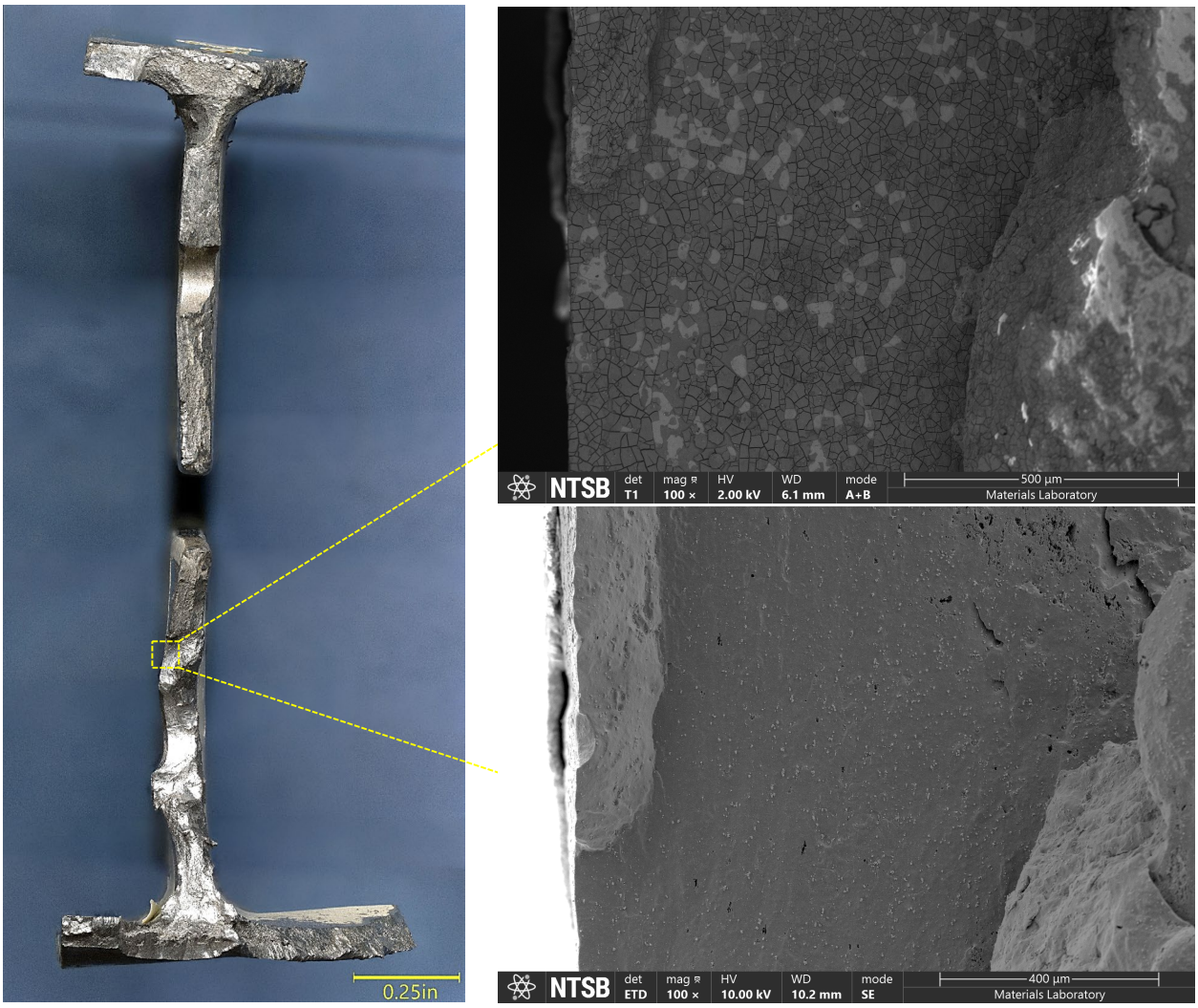

Figure 43. Scanning electron microscope images of a flatter region on the fracture surface of the lower main spar cap (outboard fracture location) before heated acid cleaning (upper right) showing a mudcracked surface consistent with a built up oxide layer from extended exposure to a marine environment. The lower right image shows the same area after heated acid cleaning and a relatively smooth and featureless appearance was observed on the fracture surface.

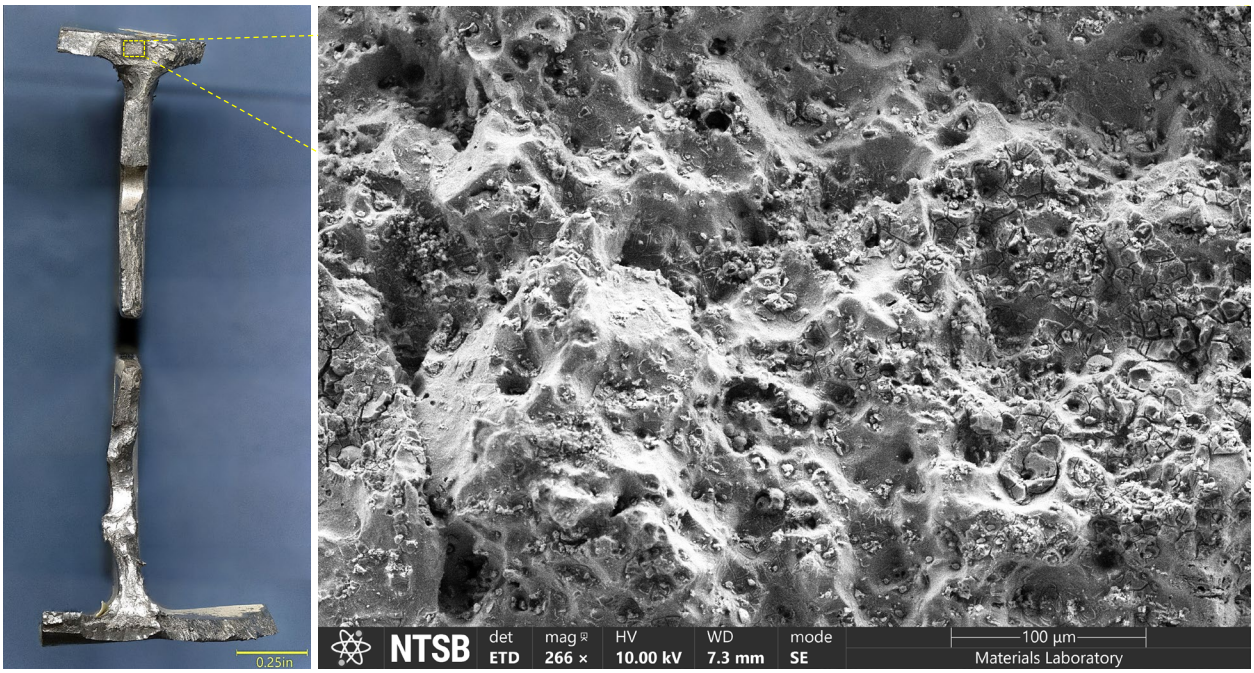

Figure 44. Secondary electron fractograph of a flatter region on the fracture surface of the upper main spar cap (outboard fracture location) showing some residual oxide layer (mudcracked appearance) over a dimpled subsurface, consistent with overstress fracture.

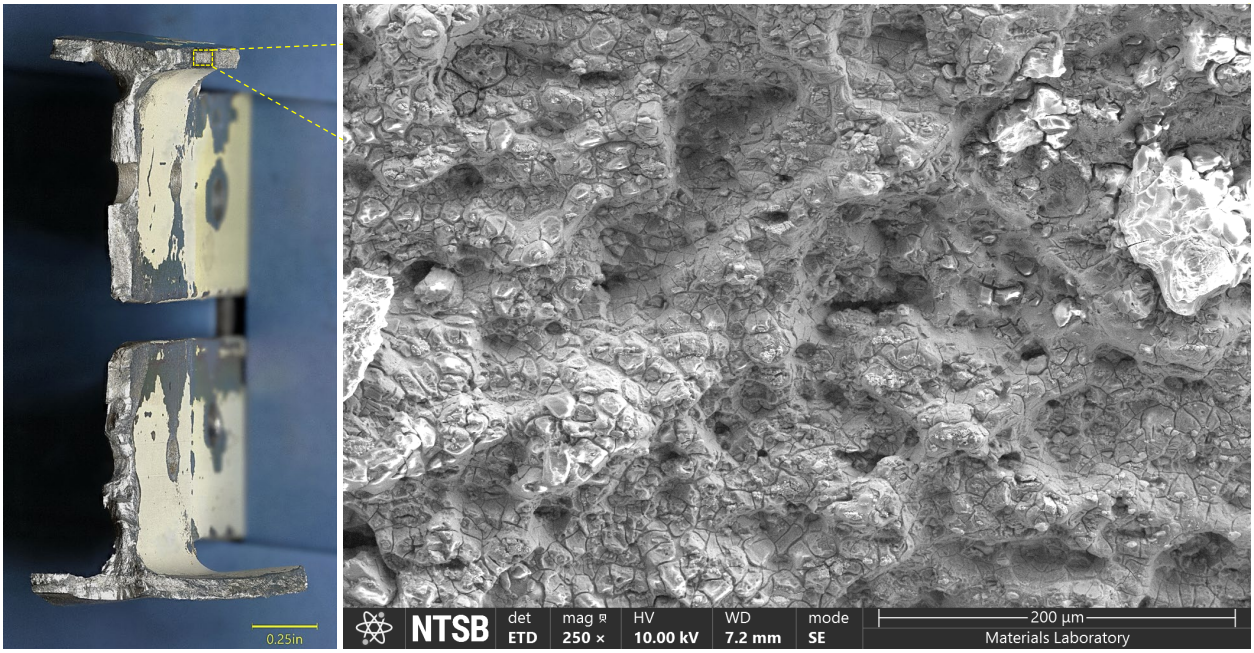

Figure 45. Secondary electron fractograph of the forward flange fracture surface of the upper main spar cap (outboard fracture location) showing an oxide layer (mudcracked appearance) over a dimpled subsurface, consistent with overstress fracture.